UNIVERSIDADE FEDERAL DE PERNAMBUCO
CENTRO DE TECNOLOGIA E GEOCIÊNCIAS
DEPARTAMENTO DE OCEANOGRAFIA
PROGRAMA DE PÓS-GRADUAÇÃO EM OCEANOGRAFIA

ISABELLE MARIA VILELA DE OLIVEIRA

DETECTION AND ANALYSIS OF THE MODES OF VARIABILITY BETWEEN SURFACE CURRENTS AND CHLOROPHYLL *a* IN THE TROPICAL ATLANTIC

Recife
2019

ISABELLE MARIA VILELA DE OLIVEIRA

DETECTION AND ANALYSIS OF THE MODES OF VARIABILITY BETWEEN SURFACE CURRENTS AND CHLOROPHYLL *a* IN THE TROPICAL ATLANTIC

Master's Dissertation presented to the Postgraduate Programme in Oceanography of the Federal University of Pernambuco as a requirement to obtain a Master's degree in Oceanography.

Concentration area: Abiotic oceanography.

Advisor: Profa. Dra. Dóris Regina Aires Veleda.
Co-Advisor: Prof.Dr. Pedro Tyaquiçã da Silva Santos.

Recife
2019

Catalogação na fonte

Bibliotecária Margareth Malta, CRB-4 / 1198

O48e Oliveira, Isabelle Maria Vilela de.
Detection and analysis of the modes of variability between surface currents and chlorophyll *a* in the Tropical Atlantic / Isabelle Maria Vilela de Oliveira. - 2019.
67 folhas, il., gráfs., tabs.

Orientadora: Profa. Dra. Dóris Regina Aires Veleda.
Coorientador: Prof. Dr. Pedro Tyaquiçã da Silva Santos.

Dissertação (Mestrado) – Universidade Federal de Pernambuco. CTG. Programa de Pós-Graduação em Oceanografia, 2019.
Inclui Referências.
Texto em Inglês.

1. Oceanografia. 2. Análise EOF. 3. Clorofila. 4. Correntes superficiais. 5. Atlântico Tropical. I. Veleda, Dóris Regina Aires. (Orientador). II. Santos, Pedro Tyaquiçã da Silva. (Coorientador). III. Título.

UFPE

551.46 CDD (22. ed.) BCTG/2019-48

ISABELLE MARIA VILELA DE OLIVEIRA

DETECTION AND ANALYSIS OF THE MODES OF VARIABILITY BETWEEN SURFACE CURRENTS AND CHLOROPHYLL *a* IN THE TROPICAL ATLANTIC

Dissertação apresentada ao Programa de Pós-Graduação em Oceanografia da Universidade Federal de Pernambuco, como requisito parcial para a obtenção do título de Mestre em Oceanografia.

Aprovada em: 08 / 02 / 2019

BANCA EXAMINADORA

_____

Profa Dra. Dóris Regina Aires Veleda (Orientador)
Universidade Federal de Pernambuco

_____

Profº. Marius Nils Muller (Examinador Interno)
Universidade Federal de Pernambuco

_____

Dr. Humberto Varona Gonzalez; (Examinador Externo)
Universidade Federal de Pernambuco

Dedico este trabalho aos meus pais, Ladjane e Samuel, à minha avó Djanira e em memória do meu avô José Vilela pelo amor e apoio que recebo ao longo da vida.

I dedicate this work to my parents, Ladjane and Samuel, to my grandmother Djanira and in memorian of my grandfather José Vilela

ACKNOWLEDGEMENTS

First, I thank God and Mary for my health and protection, and also for my family, otherwise nothing would be possible.

To my parents Ladjane Vilela de Oliveira and Samuel Gomes de Oliveira Filho, my grandmother Djanira Alves dos Santos and my grandfather José Vilela dos Santos (in memory), my grandmother Terezinha, my boyfriend Danilo Melo and my brother Rafael Vilela.

To Dr. Dóris Veleda for her friendship, orientation, confidence and encouragement, and to Dr. Pedro Tyáquiçã for all her help and co-orientation.

To the evaluating of this dissertation, my total admiration and my thanks for the suggestions to improve this work.

I thank the National Council for Scientific and Technological Development (CNPq) for the grant of the Master's Degree.

To the friends of LOFEC for the shared friendship over the years. To all the friends, lost oceanographers, from the Church, the college and the graduate of the DOCEAN for the friendship and moments of relaxation experienced whenever it was possible. To the DOCEAN teachers, who taught me a lot and shared their experiences. To the staff of the DOCEAN for the attention have given to me. Special, to thank André and Dona Edileuza.

Finally, my gratitude to all whom, in one way or another, contributed to the conclusion of this work.

ABSTRACT

The main objective of this study is to estimate and analyze the relationship of surface circulation variability with the spatial and temporal distribution of Chlorophyll *a* (Chl) in the Tropical Atlantic Ocean (TA). (1) Quantification of the main spatial and temporal variability patterns of surface currents and Chl in the TA, (2) estimative of the coupled modes of variability between surface circulation and Chl in TA. A dataset of 15-year Aqua-MODIS (Moderate Resolution Imaging Spectroradiometer) sensor data was used to determine Chl variability in the TA. In addition, 24 years of monthly surface currents data were used to investigate the main modes of variability of the surface circulation of the TA based on satellite data. The statistical method of Empirical Orthogonal Function (EOF) was applied in order to analyze the modes of Chl and surface currents variability. This study identifies the main spatial and temporal patterns of surface circulation, Chl, and the connection of Chl anomalies with the circulation of the TA through coupled modes. The EOF1 between currents and Chl (~ 25%) shows a strong covariance in the region of the equatorial divergence and the Amazon plume dispersion. The EOF2 (~ 9%) shows high covariance in the Amazon plume and, in the south, the positive anomalies are restricted to the region of influence of the Congo River. The EOF3 (~ 6%) shows an increase in the patterns of zonal current anomalies south of the equator, and at the coast of Africa, associated with a substantial increase in Chl in most of the basin. These results support future studies on large scale climate variability, thermohaline circulation, oceanic fluxes, CO_2 absorption and ecological impacts in the food chain over the TA.

Keywords: EOF analysis. Chlorophyll. Surface currents. Tropical Atlantic.

RESUMO

O principal objetivo deste estudo é estimar e analisar a relação da variabilidade da circulação superficial com a distribuição espacial e temporal da Clorofila *a* (Chl) no oceano Atlântico Tropical (AT). Para atender a esse objetivo, foram realizados: (1) a quantificação dos principais padrões de variabilidade espacial e temporal das correntes superficiais e da Chl no AT, (2) Determinação dos modos acoplados de variabilidade entre a circulação superficial e a Chl no AT. Foi utilizado um conjunto de 15 anos de dados do sensor Aqua-MODIS (Moderate Resolution Imaging Spectroradiometer) para determinar a variabilidade de Chl no AT. Além disso, foi utilizado 24 anos de dados mensais de correntes de superfície para investigar os principais modos de variabilidade da circulação superficial no AT com base em dados de satélite. Foi aplicado o método estatístico de Função Ortogonal Empírica, ou *Empirical Orthogonal Function* (EOF) a fim de analisar os modos de variabilidades da Chl e das correntes. Este estudo identifica os principais padrões espaciais e temporais da circulação superficial, da Chl e a conexão das anomalias de Chl com a circulação do AT através dos modos acoplados. O EOF1 entre correntes e Chl (~25%) evidencia uma forte covariância na região da divergência equatorial e pluma do Amazonas. O EOF2 (~9%) destaca alta covariância na pluma do Amazonas e ao sul, as anomalias positivas ficam restritas a região de influência do Rio Congo. O EOF3 (~6%) evidencia um aumento nos padrões de anomalias de correntes zonais ao sul do equador, e na costa da África, associado a um aumento substancial de Chl em quase toda a bacia.

Palavras-chave: Análise EOF. Clorofila. Correntes superficiais. Atlântico Tropical.

LIST OF FIGURES

LIST OF ABBREVIATIONS

ACT	Atlantic Cold Tongue
AC	Angola Current
AD	Angola Dome
BF	Bjerknes Feedback
Chl	Chlorophyll *a*
CI	Color Index algorithm
CNPq	Conselho Nacional Científico e Tecnológico
cSEC	central South Equatorial Current
EUC	Equatorial Undercurrent
EOF	Empirical Orthogonal Function
GC	Guinea Current
GD	Guinea Domes
HC	Heat Content
ITCZ	Intertropical Convergence Zone
MOC	Meridional Overturning Circulation
MODIS	Moderate Resolution Imaging Spectroradiometer
NBC	North Brazilian Current
NBUC	North Brazilian UnderCurrent
NECC	North Equatorial Counter Current
NEUC	North Equatorial UnderCurrent
NOAA	National Oceanic and Atmospheric Administration
nSEC	nosthen South Equatorial Current
OC3	Ocean Color version 3 algorithm
OCx	Ocean Color algorithm
OSCAR	Ocean Surface Current Analyses
PCA	Principal Component Analyses
PP	Primary Production
SCF	Squared Covariance Fraction
SEUC	South Equatorial Undercurrent
SEC	**S**South Equatorial Current
SECC	South Equatorial Countercurrent
SEC	southern South Equatorial Current

SSH	Sea Surface Height
SST	Sea Surface Temperature
SVD	Singular Value Decomposition
TA	Tropical Atlantic
TIWs	Tropical Instability Waves
UFPE	Universidade Federal de Pernambuco
WTNA	Western Tropical North Atlantic

SUMMARY

1 INTRODUCTION AND OBJECTIVES

The last decades of simultaneous satellite measurements of surface ocean circulation and Chlorophyll *a* (Chl) allow studies of air-sea interaction. Remote sensing consists of a set of capture and recording technologies of information through the absorption and emission of electromagnetic radiation (LIU, 2006; FLORENZANO, 2011; HORNING, 2018; KWOK, 2018). Consequently, it is currently possible to detect parameters derived from the ocean color, as chlorophyll and particulate matter in suspension. Remote sensing also detects surface currents, bathymetry, roughness, temperature and salinity of the surface sea (ACKER *et al*., 2003; RAJEESH and DWARAKISH, 2015). In this study, I estimated the response of distribution of the Chl concentration to surface currents in the Tropical Atlantic (TA) by the ocean color imagery.

The TA is considered an oligotrophic region limited by nutrients. The phytoplankton abundance can be estimated by measuring the Chl concentration (CULLEN, 1982), once Chl is the principal photosynthetic pigment and convenient index of phytoplankton biomass (SOLANKI *et al.*, 2001; YODER and KENNELLY, 2006). The primary production is coupled to the physical processes such as upwelling, thermocline and mixed layer depth changes, big rivers dischargers and changes in the currents variability.

The pathways and mechanisms of ocean transport are crucial issues in understanding the present state of climate and the possibilities of future changes (GANACHAUD and WUNSCH, 2000). The surface currents in TA are marked by a wide range of space-time variability. In the equatorial ocean region, for example, the variability occurs over a wide range of time and space scales, with a complex area of predominantly zonal currents, composed by westward currents and eastward countercurrents (ARNAULT and KESTENARE, 2004). The surface currents in the TA are responsible for both interhemispheric and longitudinal exchange of heat, salt, and nutrients (FOLTZ *et al.,* 2003; BRANDT *et al*., 2008; KIRCHNER *et al*., 2009).

The TA region is characterized by the presence of two broad, westward flowing currents, the South Equatorial Current (SEC) and North Equatorial Current (NEC). The SEC extends from the surface to 100m depth and it is divided into three branches: the southern South Equatorial Current (sSEC), the central South Equatorial Current (cSEC), and the northern South Equatorial Current (nSEC). Near the Brazilian coast, the sSEC bifurcates giving origin to one western boundary currents and one undercurrent: Brazil Current (BC) and North Brazil Undercurrent (NBUC) (Figure 1). The sSEC bifurcation has a climatological mean position in about 15^{o}S, with a southernmost position in July, and a northernmost in November (STRAMMA and ENGLAND 1999; RODRIGUES *et al*., 2007). The southward limb of the sSEC becomes the BC and merges into the South Atlantic subtropical gyre system. The northward limb of the sSEC flows into the NBUC (STRAMMA and SCHOTT, 1999; STRAMMA *et al*., 2005; VELEDA *et al*., 2012). The cSEC joins the NBUC near Cape São Roque in about 5^{o}S, inducing its vertical structure to change from an undercurrent to a surface-intensified current, resulting in the North Brazil Current (NBC) (Figure 1). The NBUC/NBC system supply northward warm-water, as part of the thermohaline overturning circulation (GORDON, 1986; SCHMITZ, 1995). The NBUC has a mean northward transport along the northern coastline of Brazil, with a seasonal cycle of northward flow maximum in July (SCHOTT *et al*., 2005).

The NBC flows to the northwest with maximum speeds around 1.0 m s^{-1} (RICHARDSON *et al*., 1994), with maximum transport (36 x 10^{6} $m^{3}s^{-1}$) in July – August, and minimum (13 x 10^{6} $m^{3}s^{-1}$) in April - May (JOHNS *et al.,* 1998). This current carries nutrients from the Amazon River discharge north-westward along the Brazilian shelf (MULLER-KARGER *et al*., 2005). The NBC transport is maximal when the current reaches maximum latitude and a ring is shed (GARZOLI *et al.*, 2004). The NBC dynamics produces several mesoscale rings. According to Jochum and Malanotte-Rizzoli (2003), circulation models had showed that NBC retroflection generates around 6 to 7 anticyclonic eddies per year. Theses eddies propagate northwestward along the Guyana coast (DIDDEN and SCHOTT, 1993; WILSON *et al*., 2002) by the potential vorticity conservation. The detachment of anticyclonic eddies from the NBC retroflection is observed during November through January, when the NBC retroflection flows into the NECC (DIDDEN and SCHOTT, 1993). Moreover, the NBC rings are responsible for more than half of the inter-hemispheric exchange of mass and heat

associated with Meridional Overturning Circulation (MOC) (GARZOLI *et al.*, 2003). The NBC variability is also affected by the direction of the winds in the northern Brazil. Trade winds vary seasonally along with the Intertropical Convergence Zone (ITCZ), which migrates latitudinally from March to April in around 5°S, and in August to approximately 15°N. The ITCZ drives the variability of the trade winds, mainly in the equatorial band, which are predominantly from the southeast during the June to November and from the northeast in December to May in the TA (GEYER *et al.*, 1996). When the Northeast trade winds are predominant, the NBC is confined along the coast and flows northwestward. However, during the predominant period of the Southeast trade winds, the NBC expands and retroflects eastward between 5°N and 10°N (BOURLÈS *et al*., 1999) and feeds the North Equatorial Countercurrent (NECC) (Figure 1). The NECC has eastward-transported waters, rich in nutrients, from the Amazon River plume (RICHARDSON and REVERDIN, 1987; FONSECA *et al*., 2004; COLES *et al.*, 2013). The NECC has low annual mean velocities of 5-10 x 10^{-2}ms^{-1} (RICHARDSON and WALSH, 1986), zonal current flows from west to east that varies seasonally.

The NECC flows eastward feeding the Guinea Current (GC) in the eastern TA, which is strongest in the boreal summer (LONGHURST, 1962). The GC flows eastward throughout the year, with a maximum mean velocity of 42 x 10^{-2} m s^{-1} at 4°N, 7.5°W (RICHARDSON and WALSH, 1986). At south of GC, the narrow Angola Current (AC) moves fast along the Angolan coast where it saline and warm water to coast areas (HARDMAN-MOUNTFORD *et al*., 2003) under the influence of Equatorial Atlantic variability (CHANG *et al*., 2008). Another feature near the AC is the Angola Dome (AD), which is a cold region, associated with the cyclonic turn of the South Equatorial Undercurrent (SEUC) (PETERSON and STRAMMA, 1991). The AD forms a cyclonic gyre, centred at 10°S and 9ºE, which links the South Equatorial Countercurrent (SECC) with the AC (DOI *et al*., 2007). North of the Gulf of Guinea, Bakun (1978) found a correlation between intensification of the Guinea Current (GC) and local cooling, since the GC carries cool water from the African coast to center of the basin.

The dominant seasonal SST, with low temperature in the eastern equatorial Atlantic, characterizes the formation of the Atlantic Cold Tongue (ACT) (CANIAUX *et al*., 2011). In May–June, the ACT develops rapidly when the ITCZ shifts northwards over the eastern Atlantic, with cross-equatorial southerlies intensifying, and reaches its peak in July–August (OKUMURA and XIE, 2004). The ACT is reduced through weakening of the southerly cross–equatorial winds from September onward (DEPPENMEIER *et al*., 2016). The covariability of the trade winds over the western part of the basin with SST and heat content in the eastern TA was analysed by De Almeida and Nobre (2012). These mechanisms compose the Bjerknes feedback (BF), which is responsible for the ACT mode. The ACT has a positive feedback phase peaking during boreal summer, when the Bjerknes feedback is stronger. The Bjerknes feedback consists of three components, which the first one is the influence of SST anomalies in the eastern part of the equatorial Atlantic basin on zonal winds (Bjerknes, 1969). The second is the effect of the zonal winds anomalies in the western equatorial Atlantic on the Heat Content (HC) of the eastern equatorial Atlantic, and the third one the local effect of the HC anomalies on overlying SSTs in the cold tongue region (DEPPENMEIER *et al.*, 2016).

The west and east of the TA are not independent of each other, and they are related in a high dynamic system. Strength and position of the South Atlantic anticyclone impact on timing of the ACT (CANIAUX *et al*., 2011), consequently it influences the SST variability over the TA. Moreover, the oceanic pathway consists of westward propagating of the TIWs along the equatorial Atlantic, forced by equatorial zonal wind stress anomalies (SERVAIN *et al.*, 1982; HORMANN and BRANDT, 2009).

Figure 1 – Schematic of surface and subsurface tropical Atlantic Ocean currents from MODIS/Aqua-SST. North Equatorial Current (NEC), North Equatorial Countercurrent and Undercurrent (NECC, NEUC), South Equatorial Current with northern, central and southern branches (nSEC, cSEC, sSEC), South Equatorial Undercurrent SEUC), Equatorial Undercurrent (EUC), North Brazil Current (NBC), North Brazil Undercurrent (NBUC), GD (Guinea Domes), Angola Domes, and the NBC anticyclonic ring (R) displacement. Colored map represents the average SST (June, July and August 2009).

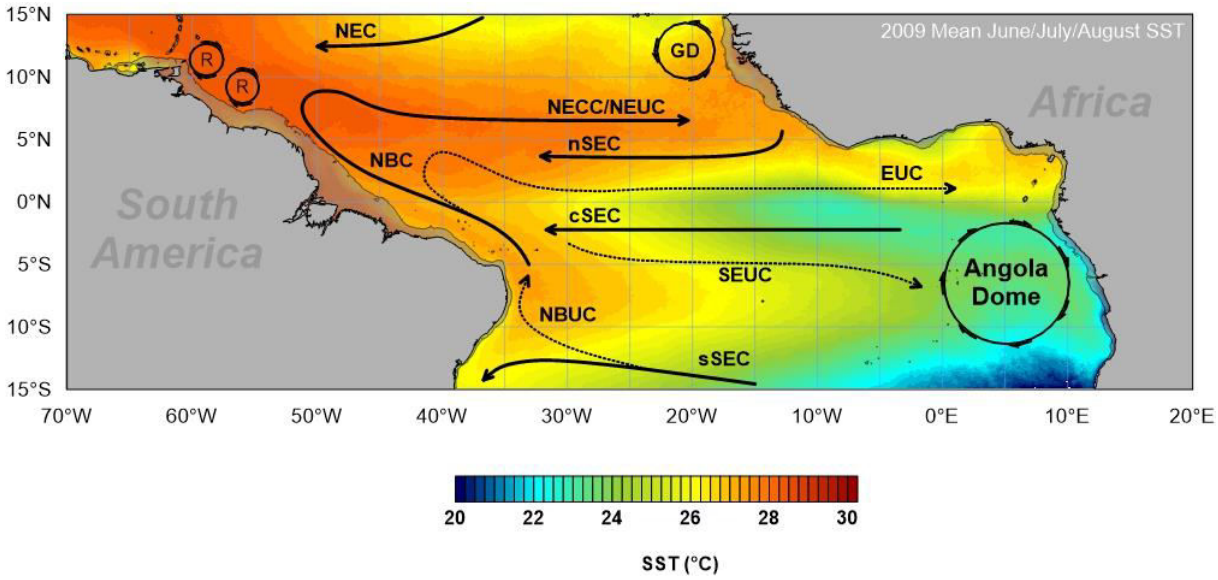

Source: The Author

The main objective of this study is to estimate and analyse the response of the spatial and temporal distribution of Chl to the surface circulation of the Tropical Atlantic Ocean. To achieve this purpose, specific goals were performed: (1) quantifying the main patterns of variability of the surface currents and Chl in the Tropical Atlantic. (2) analysing the oceanographic processes that command the variability of currents and Chl in the Tropical Atlantic and assess the relationship of these variables. This work brings an overview of the study area, a description of the analysis tools, the results and discussion are presented through two manuscripts submitted to scientific journals, as the main conclusions and perspectives.

2 THE STUDY AREA

This study focuses on the TA, comprised the region from 20°S to 20°N in latitude, and from 70°W to 20°E in longitude (Figure 2). The purpose here is to introduce the area of study with a view of the main physical characteristics that influence the dispersion of Chl in the TA. The Chl concentration is high along the coast region, mainly due to the contribution of the large rivers, and the upwelling areas (Figure 2).

The large rivers discharges are a very important nutrients source into the ocean, increasing phytoplankton biomass and can lead to substantial CO_2 uptake (KÖRTZINGER, 2003; REGNIER *et al*., 2013). In the TA the largest rivers discharges are: Amazon, Orinoco and Congo plumes. The Amazon River is the largest terrestrial freshwater source for the Atlantic, which contributes with 20 – 30% of the total fluvial flow (WISSER *et al*., 2010). The Amazon minimum discharge is in November (~0.8 x 10^5 m^3s^{-1}) and maximum, in late May (2.4 x 10^5 m^3s^{-1}) (LENTZ, 1995). The Orinoco is the third largest river in the world, with discharges of approximately 0.03 × 10^6 m^3s^{-1} (PERRY *et al*., 1996; DAGG *et al.*, 2004), and the Congo plume extends hundreds of km offshore (DENAMIEL *et al*., 2013; HOPKINS *et al.,* 2013).

In the TA are three significant areas of upwelling: coastal Senegalo-Mauritanian upwelling, northern Gulf of Guinea, coastal upwelling of Benguela and the equatorial divergence. Upwelling is subsurface waters, cold and rich in nutrients ascend to the surface, which provides a good condition for phytoplankton growth. The highest Chl concentration (Figure 3) along the African cost is associated with the upwelling phenomenon in the east coast and the equatorial divergence. Further northwest, in the Senegalo-Mauritanian upwelling region, the wind regime is responsible for quasi-permanent Ekman pumping and coastal upwelling between the Cape Verde frontal zone (~21°N, Mauritania) and the Cape Verde Archipelago and Cape Roxo (~12°N) (CAPET *et al.*, 2017). In the northern Gulf of Guinea, the cooling has been correlated with the Guinea Current intensification (BAKUN, 1978), and at the equator it is forced by wind regime (PICAUT, 1983). The Benguela

upwelling occurs along shore due to the winds stress, that generally peaks in the warm season and east boundary currents (CHAVEZ and MESSIÉ, 2009).

Figure 2 – Schematic representation of the main surface currents in the study area. A MODIS/Aqua Chl image of the period Jul/2002 to Oct/2018 is used to highlight the largest discharges of rivers in the TA and regions of upwelling.

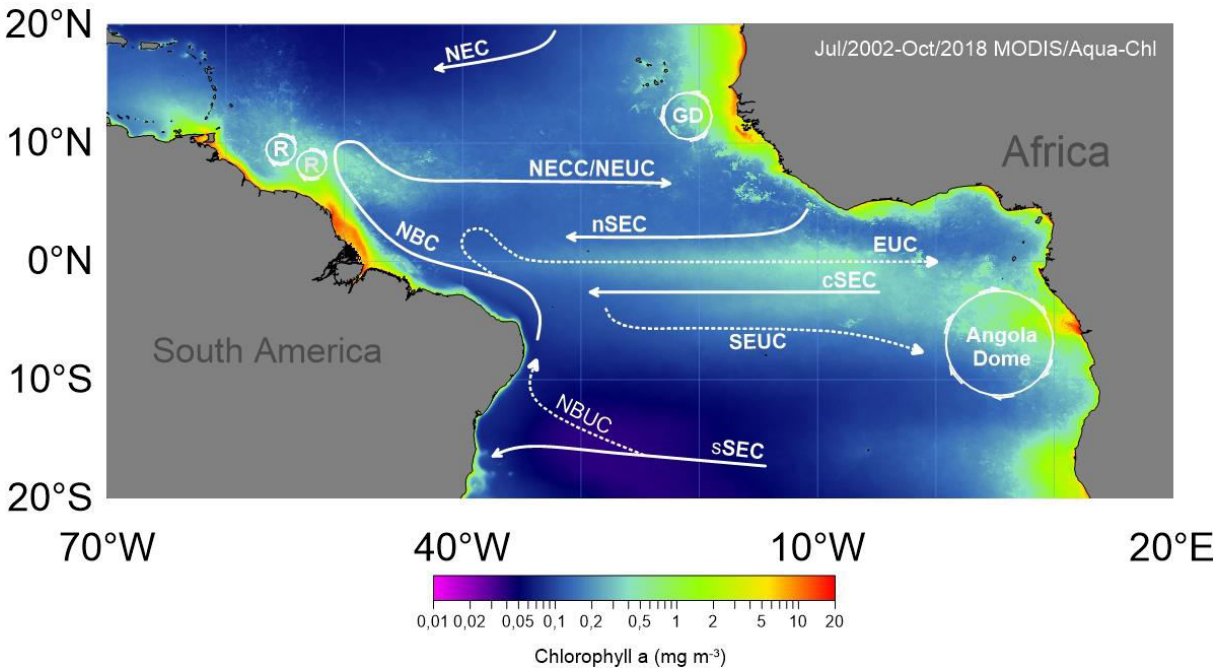

Source: The Author

Climatologically, the Chl is confined to the continental shelf along the South American coast during December, January and February (Figure 3a) from 2003 to 2017, where the maximum Chl concentration is over the Amazon plume region. The Amazon plume is influenced by the North Brazilian Current (NBC) that carries nutrients from this river to the northwest along the Brazilian Shelf (MULLER-KARGER *et al.,* 1988). Ffield (2005) identified that the Amazon River freshwater flows northwest, merging with the Orinoco River plume from July to December (LENTZ and LIMEBURNER 1995; LENTZ 1995).The Amazon plume has a great influence on the north of the South American coast, the Equatorial Atlantic Ocean and the Caribbean, in regard to phytoplankton biomass (SMITH and DEMASTER, 1996). In March, April and May the Chl climatology extends beyond the continental shelf in the northwestward direction (Figure 3b) along the NBC flow. However,

from June to August (Figure 3c) the Chl concentration extends beyond the continental shelf in a retroflection pattern towards eastward direction. In September, October and November climatology, the Chl concentration is high along the NBC retroflection that carries nutrients from the Amazon plume (Figure 3d). During the austral spring through fall, when the retroflection of the NBC takes place and during high-discharge periods, the Amazon plume reaches 3°N – 10°N, and it is carried eastward by the NECC (FRATANTONI and GLICKSON, 2002).

In eastern of the basin, the Congo River contributes to the discharge of nutrients in the TA, which the maximum flow occurs in November-January with plume extending hundreds of km offshore (DENAMIEL *et al*., 2013; HOPKINS *et al.,* 2013). Likewise, the Figure 3a shows a maximum Chl concentration at the Congo plume in about 6ºS. Moreover, according to Jouanno (2011), at 4°S and 5°E a maximum pattern of Chl is associated with Congo River plume and coastal upwelling (SIGNORINI *et al*. 1999).

The figure 3c shows a well-defined pattern of the Chl climatology, and the Chl dispersion westward along the ACT region under the influence of surface currents and trade winds. The ACT develops over the eastern Atlantic, with the cross-equatorial southerlies intensifying in July–August (OKOMURA and XIE, 2004), as shown in the figure 3c, but it is reduced from September onward (DEPPENMEIER *et al*, 2016). The ACT develops rapidly when the ITCZ shifts northward over the eastern Atlantic in May–June with cross-equatorial intensified southerlies. The ACT peak is in July–August (OKUMURA and XIE, 2004), and it is reduced from September onward (DEPPENMEIER *et al,* 2016). Consequently, the seasonal main peak of Chl concentration occurs in June to August and the secondary in December, also the highest concentrations cover the area from 20°W to 10°W and between 1°S to equator (JOUANNO, 2011).

Figure 3 – SeasonalChlorophyll *a* climatology from 2003 to 2017 (a) December, January and February, (b) March, April and May, (c) June, July and August, (d) September, October and November, for the study area.

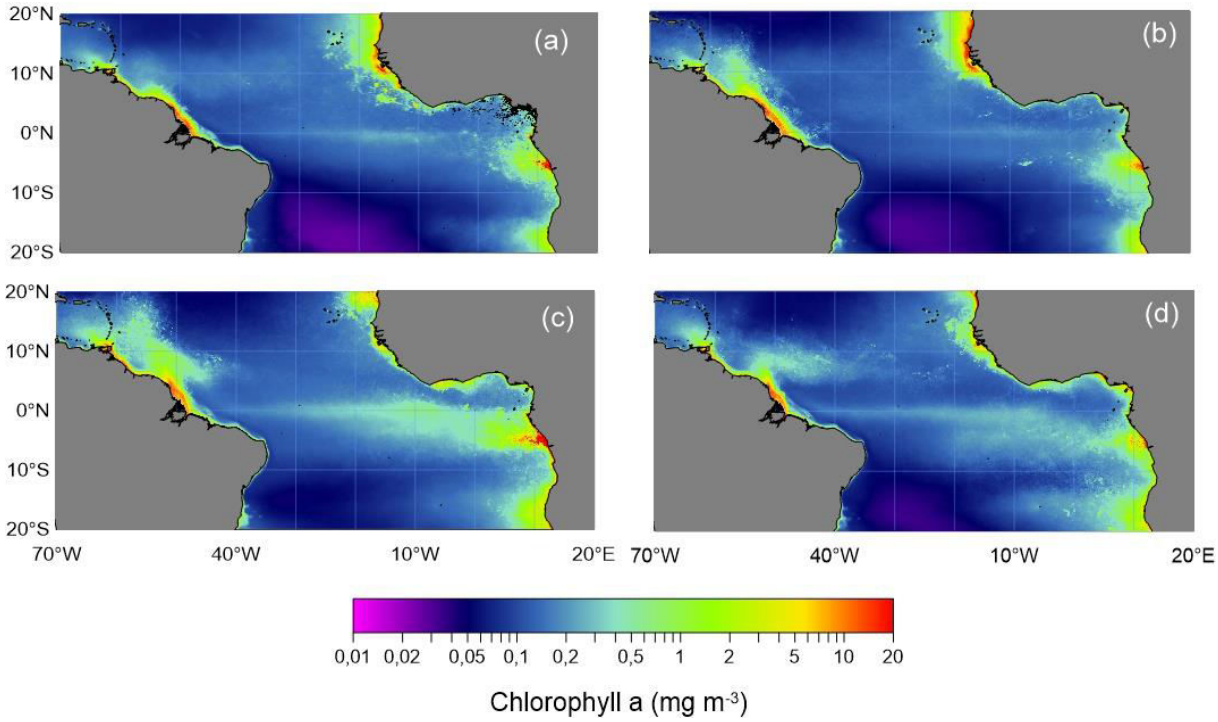

Source: The Author

3 DATA AND METHODS

In the present study, I used data of surface currents, zonal and meridional components and Chl over the TA in order to analyze the mean modes of variability.

3.1 DATA

Surface currents

The knowledge of the zonal (u) and meridional (v) components of the surface currents are very important to understand the ocean dynamics. The study of surface current contributed for many oceanographic applications, which are necessary for monitoring the role of horizontal advection on plankton dynamics (GARÇON *et al*., 2001) and its dispersion along the ocean. One database of surface currents applied in this study is from satellite data. The surface currents are a direct computation of global surface currents using satellite Sea Surface Height (SSH), wind-driven, and Sea Surface Temperature (SST). The model calculates a surface current averaged over the top 30m of the upper ocean, using a quasi-steady geostrophic model together with an eddy viscosity based wind-driven geostrophic component and a thermal wind adjustment. Besides that, a dynamically improved model for the equatorial region has been developed and implemented in the 1/3 degree OSCAR (Ocean Surface Current Analyses) system, and many smaller-scale features are now observable in the higher resolution model. The area used for the analysis of the surface circulation is comprised to the region of 20°S and 20°N, 70°W and 20°E in the Tropical Atlantic. Data from January 1993 to December 2017 was used on a 1/3° grid and obtained from the Ocean Surface Current Analyses OSCAR/NOAA (National Oceanic and Atmospheric Administration) archives resolution (http://www.oscar.noaa.gov).

The OSCAR project attempts to better understand air-sea momentum exchange using satellite observations with simplified physics to calculate global ocean currents (DOHAN, 2017). OSCAR currents combine Ekman and geostrophic currents based on QuikSCAT (Quick Scatterometer) winds, and TOPEX (Topography Experiment). Poseidon sea level

height measurements (BONJEAN and LAGERLOEF, 2002). Johnson *et al.* (2007) found that the OSCAR product provides accurate estimates of zonal and meridional time-mean circulation, and in the near-equatorial region reasonably accurate estimates of zonal current variability, when comparing with moored current meters, drifters, and shipboard acoustic doppler current profiler (sADCP) instruments.

Chlorophyll *a* (*Chl*)

The phytoplankton biomass has been studied as a key component in the oceanic carbon cycle and the Earth's climate system (BEHRENFELD and FALKOWSKI, 1997). Spatial patterns of Chl distribution in the surface ocean are a result from regional and global physical processes, which influence on the phytoplankton growth. Chl concentrations have typically been the main biophysical variable derived from satellite imagery. The ocean color imagery has proven to be effective for deriving biophysical variables as the ocean phytoplankton, at temporal and spatial scales, which are difficult to obtain with oceanographic surveys (SATHYENDRANATH *et al*., 2001).

Chl concentration images by the MODIS (Moderate Resolution Imaging Spectroradiometer) sensor produced by NASA Ocean Color Group are based on the OC3 (Ocean Color version 3) algorithm that returns the near-surface Chl concentration in mg m^{-3}. This algorithm is calculated using in situ measurements of Chl and remote sensing reflectances (*Rrs*) in the blue, green and red bands (O'REILLY *et al*., 1998). The Chl algorithm product employs the OC3/OC4 (OCx) band ratio algorithm merged with the color index (CI) of Hu *et al*. (2012). The CI algorithm is a three-band reflectance difference algorithm formed between the *Rrs* in the blue, green and red bands, as follow:

$$\boldsymbol{CI = Rrs\,(\lambda_{green}) - [Rrs\,(\lambda_{blue}) + \frac{(\lambda_{green} - (\lambda_{blue})}{(\lambda_{ref} - (\lambda_{blue})} * (\,Rrs\,(\lambda_{red}\,) - \,(\lambda_{blue})\,]} \qquad \textbf{(1)}$$

Respectively the λ_{blue}, λ_{green} and λ_{red} are the instruments-specific wavelengths closest to 443, 555 and 670 nm. The Chl in logarithmic scale is derived by the OCx algorithm, which it is a fourth-order polynomial relationship between a ratio of *Rrs* and Chl.

$$\boldsymbol{log_{10}(Chl) = a_0 + \sum_{i=1}^{4} a_i \left(log_{10} \left(\frac{Rrs\,(\lambda_{blue})}{Rrs\,(\lambda_{green})} \right) \right)^i} \quad \textbf{(2)}$$

Where the Rrs (blue and green) values and the coefficients (a_0 to a_4) are sensor- specific.

Monthly composites of Chl obtained from the Aqua MODIS sensor with spatial resolution of 4 km were downloaded from the NASA web server (accessible at https://oceandata.sci.gsfc.nasa.gov/MODIS-Aqua/), covering the period of January 2003–December 2017.

3.2 ANALYSIS TOOLS

Analysis Tools Climatology is commonly used as the study of our climate. The monthly climatology produces a mean value for each month, over a specified time range. The interannual variability is analysed from anomalies, which are calculated by subtracting monthly climatological values from observed data, as follow:

$$\boldsymbol{Anomaly = Xobs - \overline{Xclimatology}} \quad \textbf{(3)}$$

3.2.1 Wavelet Analysis

To analyse the time series was applied the wavelet analysis, which provides a suitable tool for non-stationary series. The wavelet detects the intermittent periodicities in the time–

frequency domain. Kumar and Foufoula-Georgiou (1997) described the geophysical applications and Daubechies (1992, 1999), a theoretical treatment of wavelet analysis.

3.2.2 Empirical Orthogonal Function analysis (EOF)

The EOF is often used to identify the main modes of variability in climate studies, once the interactions between physical processes in the atmosphere-ocean system are operate on a wide range of data, with large spatial and temporal scales.

The EOF decomposes a multivariate data set into modes, which represent variability in time and space from the original data, a method based on multivariate analysis. This statistical method is used to extract intrinsic characteristics in which vary spatially and temporally reducing several dimensions into a few (WILKS, 1995).

To calculate the EOF it is necessary to transform the data matrix into three dimensions, considering N maps for each time $t=1...N$, where each map contains location measurements $m = 1 \ldots M$, since all locations also contribute to the analyses. The spatial matrix M has latitudes and longitudes, forming a tri-dimensional matrix with time N, f = *[latitudes x longitudes x time]*. Besides that, it is necessary to perform combinatorial analysis in matrix f between latitudes and longitudes, in order to create another matrix F with two dimensions ($F = M \times N$), as follow:

$$F = \begin{bmatrix} F_1(1) & F_1(2) \ldots & F_1(N) \\ F_2(1) & F_2(2) \ldots & F_2(N) \\ \cdots & \cdots & \cdots \\ F_M(1) & F_M(2) \cdots & F_M(N) \end{bmatrix} \quad \textbf{(4)}$$

Where M rows represents the position m, and N columns represent time (t).

The covariance matrix (*Cov*) is calculated by the matrix *F* multiplied to its transpose F', as follow:

$$\boldsymbol{Cov = F * F'} \quad \textbf{(5)}$$

$$\boldsymbol{Cov} = \begin{bmatrix} < F_1F_1 > & < F_1F_2 > & \cdots & < F_1F_M > \\ < F_2F_1 > & < F_2F_2 > & \cdots & < F_2F_M > \\ \cdots & \cdots & \cdots & \cdots \\ < F_NF_1 > & < F_NF_2 > & \ldots & < F_NF_M > \end{bmatrix} \quad \textbf{(6)}$$

The linear combination *<F_iF_j>* is the covariance between the time series *Fi* and *Fj*, where *i, j =1...M* is the location in the matrix, calculated by the equation:

$$< F_iF_j > = < F_jF_i > = \frac{1}{N-1}\sum_{t=1}^{N} F_i(t)F_j(t) \quad \textbf{(7)}$$

The Singular Value Decomposition (SVD) method calculates eigenvectors and their corresponding eigenvalues (YODER *et al*., 2003).The SVD is based on the concept that any matrix *M* x *N* can be written by the product of three matrices: a matrix *U (M* x *M),* one diagonal matrix *S (M* x *N)* and one transposed matrix *(V')* of the matrix *V (M* x *N)*. The SVD is calculated as follow:

$$\boldsymbol{F = U * S * V'} \quad \textbf{(8)}$$

To perform the matrix $\boldsymbol{A}$:

$$\boldsymbol{A = S * V'} \quad \textbf{(9)}$$

Resulting in a matrix *A* that contains the diagonal of eigenvalues λ_k:

$$\boldsymbol{A} = \begin{bmatrix} \boldsymbol{\lambda_1} & \mathbf{0} & \cdots & \mathbf{0} \\ \mathbf{0} & \boldsymbol{\lambda_2} & \cdots & \mathbf{0} \\ \cdots & \cdots & \cdots & \cdots \\ \mathbf{0} & \mathbf{0} & \cdots & \boldsymbol{\lambda_k} \end{bmatrix} \quad \textbf{(10)}$$

Each eigenvalue λ_k is proportional to the percentage of the variance of *F*, being represented by the mode *k* as follow:

$$\boldsymbol{\sigma_k} = \%\, \boldsymbol{variancemodek} = \frac{\boldsymbol{\lambda_k}}{\sum_{i=1}^{k} \boldsymbol{\lambda_i}} * \mathbf{100} \quad \textbf{(11)}$$

In general, each *k* mode accounts for a variance σ_k, where λ_k is the eigenvalue of the k[th] eigenvector. The projecting coefficients obtained by the expansion of the sample data to the eigenvectors are the principal components, also called expansion coefficients (VAUTARD *et al*., 1992).

The EOF generates modes of variability where, the first mode (EOF1) represents the maximum fraction of the total variance and its first Principal Component (PC1) is the time evolution associated to this pattern. The second mode (EOF2) is unrelated to the EOF1, represented by the largest variance of the remaining dataset. In the third mode (EOF3), similarly, there is not related to the previous modes (EOF2 and EOF1). Thus, the principal components (PC1, PC2 and PC3 …PC*n*) are associated to the temporal patterns for each mode (EOF1, EOF2, EOF3 … EOF*n*), representing the variability of spatial modes in the time (WILKS, 1995).

4 RESULTS AND DISCUSSION

The results are presented in three sessions (4.1, 4.2 and 4.3). The sections 4.1, 4.2 show the results from two scientific articles produced throughout the present study, the first one about surface currents modes and the second one about Chl modes in TA. The last section, 4.3, shows the final results about the coupled mode between surface currents and Chl.

4.1 EMPIRICAL ORTHOGONAL FUNCTION ANALYSIS OF SATELLITE-DERIVED CURRENTS IN THE TROPICAL ATLANTIC

The EOF analysis was applied to 24 years of current speed, zonal and meridional components, which allows identifying the main space-time variability in the TA through the EOF analysis. The EOF mode and its respective PCs were performed to the surface current velocities as to the zonal and meridional components. In this section, the results are restricted to 15^{o}S to 15^{o}N in the TA, which was necessary due to computational limitation. The analysed results allowed quantifying the main modes of surface currents in the TA. Associated to each PC I perform the wavelet analysis to detect the main patterns of variability.

EOF ANALYSIS OF THE MERIDIONAL COMPONENTS

Figures 4-6 represent the main patterns identified in the meridional component. In the EOF1, the meridional component explained 18.77% of the total variance (Figure 4).

Figure 4 – First EOF mode of 24 years of the surface meridional component, the SCF in percentage, and the first PC1.

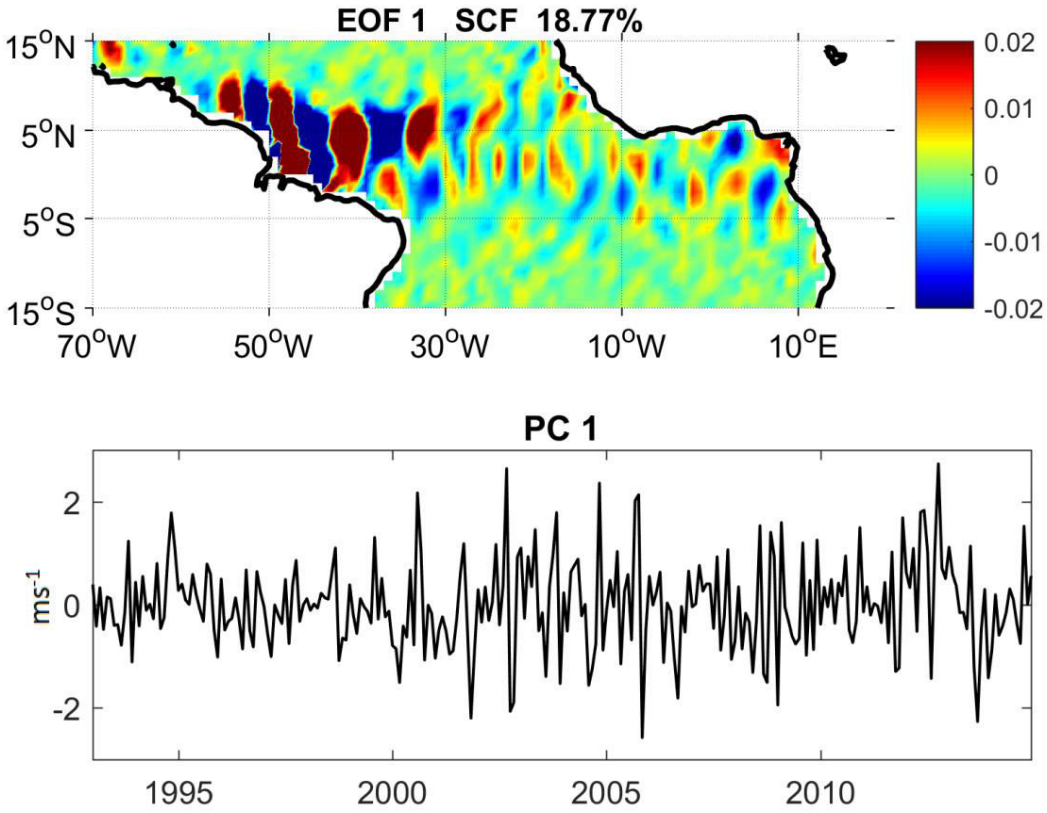

Source: The Author

The main characteristic of the EOF1 shows a spatial pattern with alternating positive and negative cores of the meridional component. This pattern is confined to the Western Tropical North Atlantic (WTNA), which is a region characterized by strong variability of the NBC retroflection and rings (JOHNS *et al.*, 1998). These structures indicate the high variability of this region, associated to NBC retroflection and rings detachments, as well its westward propagations along the Guyana coast (DIDDEN and SCHOTT, 1993; WILSON *et al.*, 2002). In approximately 50°W, where there is the Amazon River, I identify a negative core (southward movement) at the west of the river mouth and a positive core at the east. These alternating cores reach approximately 55°W, which is a predominant limit identified as the NBC retroflection (JOHNS *et al.*, 1990; FRATANTONI and GLICKSON, 2002). In the eastern Tropical Atlantic this pattern weakens, and it is not well defined as in the western basin.

The spatial pattern of EOF2 of the meridional component (Figure 5) corresponded to 11.98% of the covariance. As in the EOF1, the main characteristic of the second mode shows a spatial pattern of alternating positive and negative cores, also confined to the WTNA, however expanding and weakening towards the eastern Atlantic. I identify a positive core (northward movement) at the river mouth position, followed by negative core displaced to the west. The last positive core more west can indicate the NBC retroflection, in this case positioned approximately at 60ºW. Comparing the last positive core at west in the WTNA, in the EOF2, with the respective position in EOF1, I identify a westward shift of these alternating signals. The eastern part of the basin shows similar pattern, but weaker in comparison with the WTNA. Nevertheless, the EOF2 exhibits stronger variance in the eastern basin than in the EOF1. The spatial pattern of the second mode in the east side of the basin is well defined, with alternating positive and negative signals, confined between 5°S and 5°N.

Figure 5 – Second EOF mode of 24 years of the surface meridional component, the SCF in percentage, and the PC2.

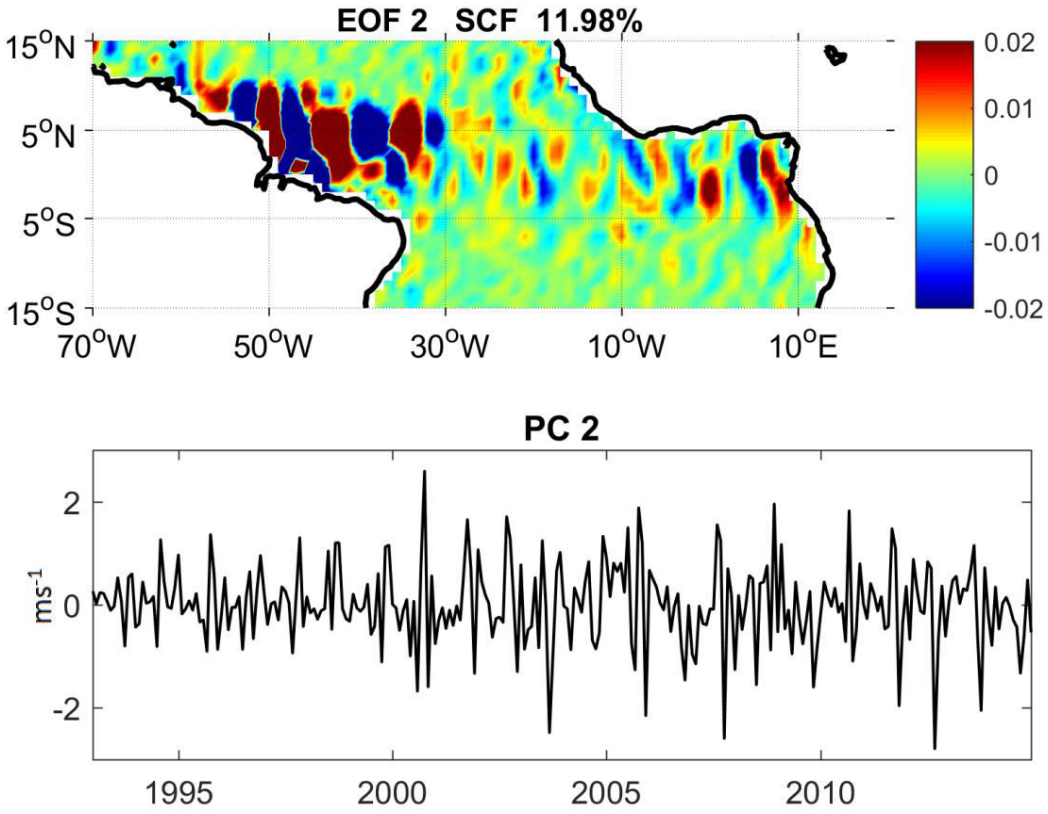

Source: The Author

The EOF3 explained 10.29% (Figure 6) of the total variance. Similar to the first modes 1 and 2, the main spatial pattern of the third mode also shows alternating positive and negative cores in the WTNA. I identify a negative core at the east of the river mouth position, followed by positive core in the west. In this case, high variance exists to the west, with continuous alternating positive and negative signals. The eastern part of the basin shows alternate pattern, but not well defined as in comparison with EOF2.

The EOF4 of the meridional component corresponded to 8.97% (not showed), EOF5 retains 5.57% of the total variance (not showed) and showed similar pattern to the EOF1. In these modes, I identify the low variance with too continuous alternating cores of positive and negative values, along the equatorial region. However, these structures are better defined in the three first modes. The PCs are associated with each mode, they showed very similar pattern with high frequency oscillations.

Figure 6 – Third EOF mode of 24 years of the surface meridional component, the SCF in percentage, and the PC3.

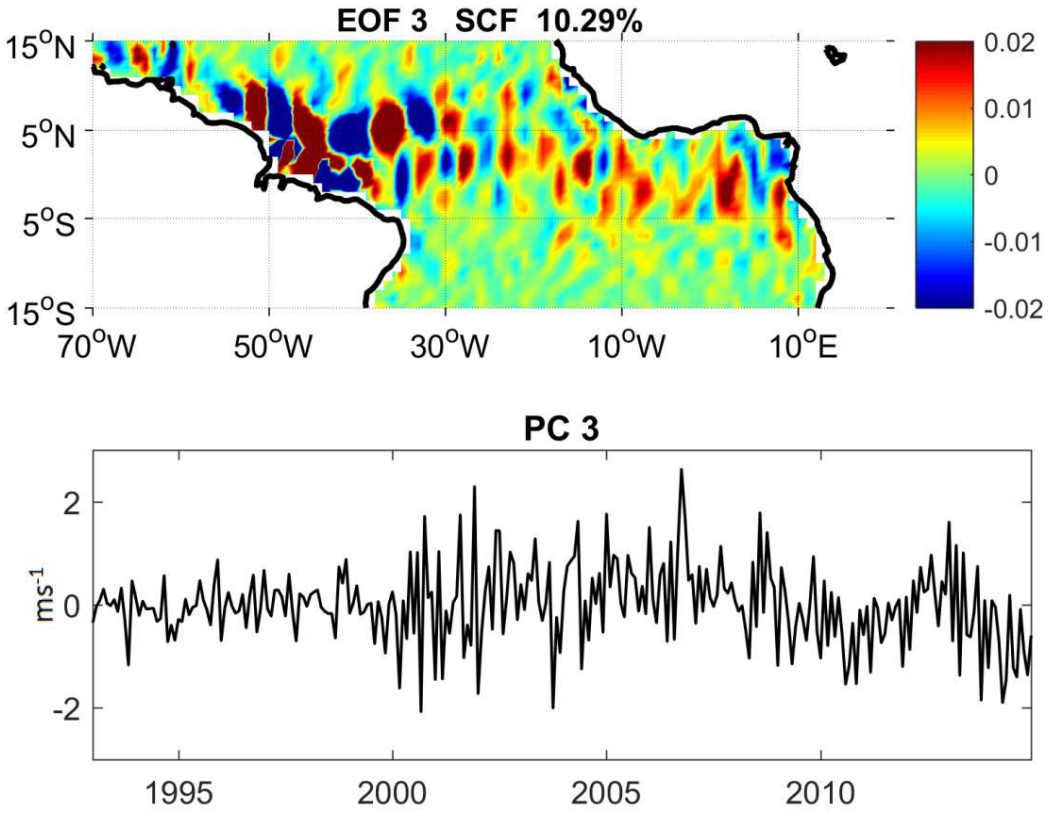

Source: The Author

The main difference between these signals in the WTNA, in the modes 1 to 5, is the zonal shift of these structures and their relative intensities, corroborating with the high dynamics identified in this region, as the NBC retroflection (east to 7ºN and 52ºW) and formations of anticyclonic eddies. Except in the EOF2 and EOF5, where visible structures of opposite signals are stronger and evident. In the EOF5 the structures in the eastern basin are strong, well defined and they propagate across the Atlantic basin, interacting with the WTNA structures. Despite these patterns in the eastern part of the basin have been detected with monthly data, they present structures like TIWs. According Legeckis (1977) and Legeckis *et al*. (1983) the TIWs have a wavelength of about 1000 km and a period of 30 days. Also, Evans *et al*. (2009) have identified these structures using monthly SST and chlorophyll data. Therefore, these structures found in EOFs 1 to 5 present the same pattern found in Decco *et al.* (2016). The TIWs propagate westwards of the thermal equator (DECCO *et al*., 2016), loading energy as heat from tropical regions to other regions of the world (COX, 1980; WEISBERG and HORIGAN, 1981). Sea level fluctuations associated with TIWs are strong in the regions between 2^{o}N to 5^{o}N and 2^{o}S to 5^{o}S, and at west of 10^{o}W (HAN *et al*., 2008; VON SCHUCKMANN *et al*., 2008).

WAVELET ANALYSIS OF THE MERIDIONAL COMPONENTS

For extracting more information about the variability of the principal components, the wavelet analysis is applied and identifies the dominant periodicities from the PCs for the meridional component. The wavelet analyses of the PCs 1, 2 and 3 (Figure 7) exhibit the periodic components of variability in the time series.

The wavelet of the PC1 showed a strong peak in the variance in 2000 with periodicity about 12 months and intraseasonal peaks in 2002, 2003, 2005, 2008 and 2012. The PC2 showed intraseasonal peaks between 2002, 2003, 2005, 2007, 2011, 2012. A strong and continuous variance signal with about 36 month-period is identified in the years from 2002 to 2008. In the PC3 the strong intraseasonal variance is identified in 2001/2002 and strong annual anomalous signal between 2003 and 2004 and 2007/2008.

Figure 7 – The wavelet transform of the Principal Components (PC1, PC2 and PC3) from the EOF1, EOF2 and EOF3 respectively of the meridional component along the Tropical Atlantic.

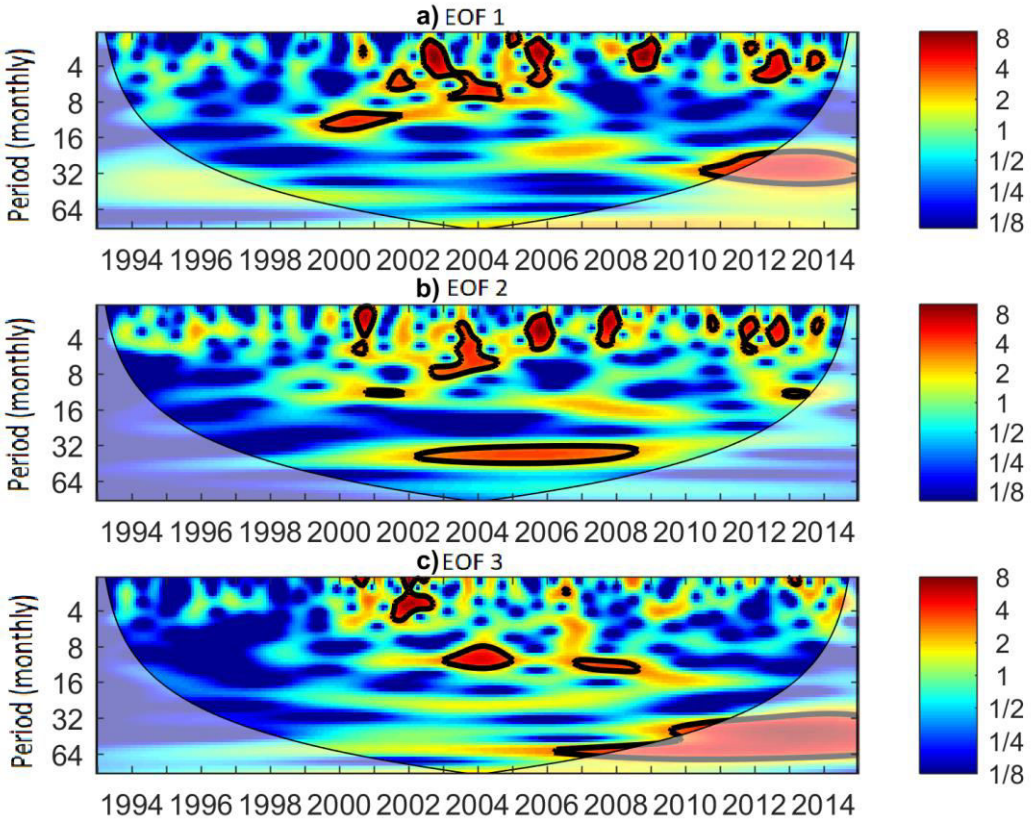

Source: The Author

EOF ANALYSIS OF THE ZONAL COMPONENTS

The following results (Figures 8, 9, 10) show the EOF analysis of the zonal components. The EOF of the first three zonal components account for more than 80% of the total variance.

The EOF1 corresponded to 50.73% of the total variance (Figure 8). The spatial pattern shows a negative signal between 5°S - 5°N, which cover the cSEC position (3° - 5°S). This large and negative signal is associated with the central branch of the cSEC and part of this negative pattern also covers the area of the northern nSEC, which is about 2ºN and 3°N (URBANO *et al.,* 2008). This negative signal also flows along the north of Brazilian coast, representing the NBC. Further north, between 5ºN-7°N, the EOF1 shows a positive signal flowing eastward, from approximately 51°W to 12°E (Figure 8), which can be associated to

the NECC position. The NECC flows generally eastward between about 3ºN – 10ºN (HORMANN *et al*., 2012), bounded at north by the westward North Equatorial Current (NEC) and at the south by the westward nSEC.

Figure 8 – First EOF mode of 24 years of the surface zonal component, the SCF in percentage, and the PC1.

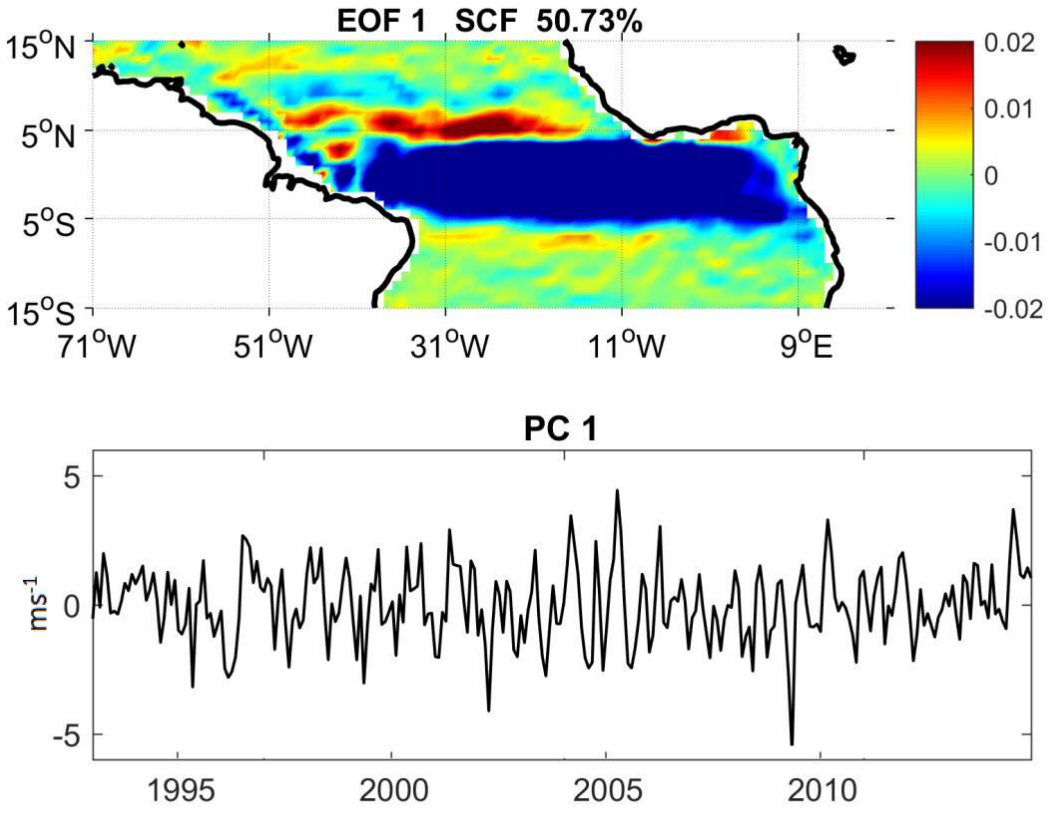

Source: The Author

The EOF2 of the zonal component explained 8.23% of the total variance (Figure 9). The EOF2 shows a positive signal in the WTNA. This positive signal exists along the north Brazil coast. North of the positive signal in the WTNA, there is a negative signal approximately 7°N - 8°N, which is associated with the NECC. In other words, the EOF2 shows a zonal dipole with a positive signal in the west and a negative in the eastern TA. The negative signal in the eastern TA covers the area of the cold tongue, near African coast. The formation of the ACT is the dominant seasonal SST signal in the eastern equatorial Atlantic (CANIAUX *et al*., 2011). This zonal dipole is associated with the BF, once the BF is stronger when the cold tongue shows a positive phase peaking during boreal summer (De ALMEIDA and NOBRE, 2012; DEPPENMEIER *et al.,* 2016).

The ACT reaches its peak in July–August (OKOMURA and XIE, 2004), from September onward, the upwelling is reduced through weakening of the southerly cross–equatorial winds (DEPPENMEIER *et al.*, 2016). De Almeida and Nobre (2012) have analysed the covariability of the trade winds over the western part of the basin, with SST and heat content in eastern TA. These mechanisms compose the Bjerknes Feedback (BF), which is responsible for the ACT mode. The ACT has a positive feedback phase peaking during boreal summer, when the BF is stronger. The negative signal identified in the eastern TA (Figure 9) evidences that, it could be a response to the first BF component, once that the westward zonal currents are forced by the intensification of the southeasterly winds. Also, the strongest variance in the PC2 of the zonal component coincides with a negative phase of the Atlantic Niño in 2004-2005. Besides that, the positive signal in the west (Figure 9) shows an inverse signal, associated to the warm pool region.

Figure 9 – Second EOF mode of 24 years of the surface zonal component, the SCF in percentage, and the PC2.

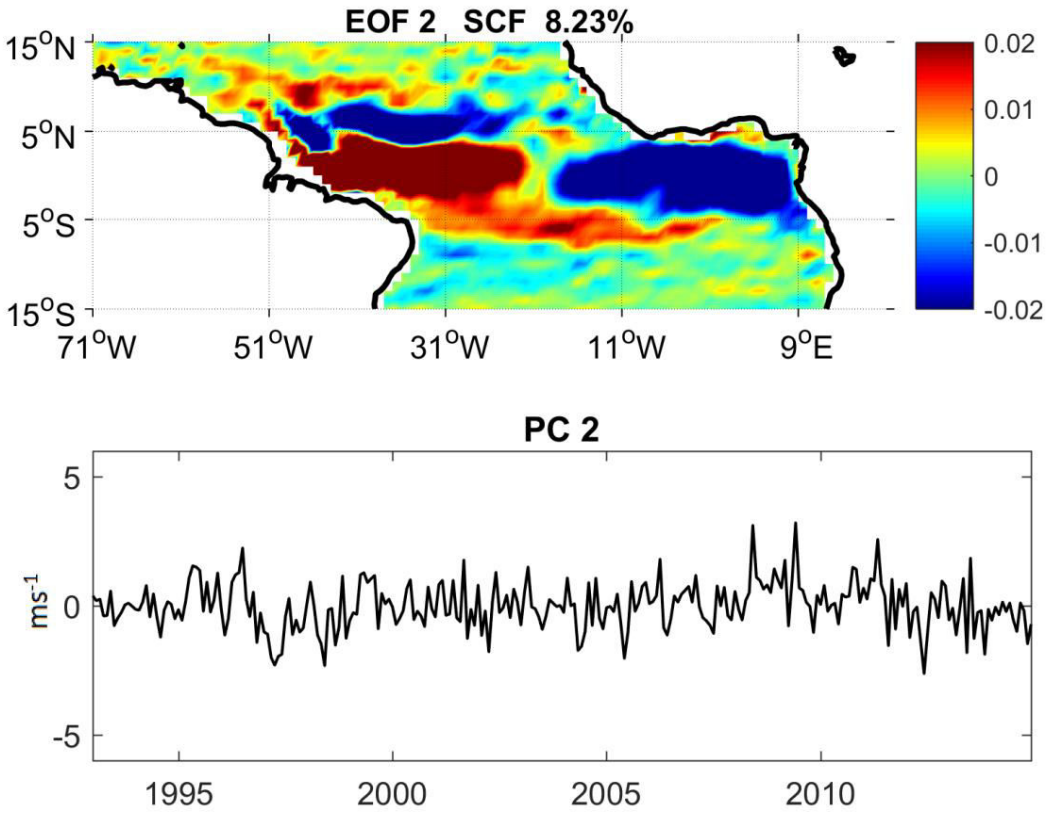

Source: The Author

The EOF3 represents 5.67% of the total variance (Figure 10). Approximately between 3°S and 5°N, a predominant negative signal, indicating a westward flow, crossing the Atlantic basin, and then flowing north-westward along the north Brazil coast, as the NBC position. Further South, between 3°S - 5°S, a positive signal indicates eastward flow, from the Brazilian coast to African coast. In this case, this signal could be related to a meridional shift of the cSEC. At north, the positive signal is established at 5°N -7°N approximately from the 50°W to 10°W (Figure 10), related to the NECC position.

Figure 10 – Third EOF mode of 24 years of the surface zonal component, the SCF in percentage, and the PC3.

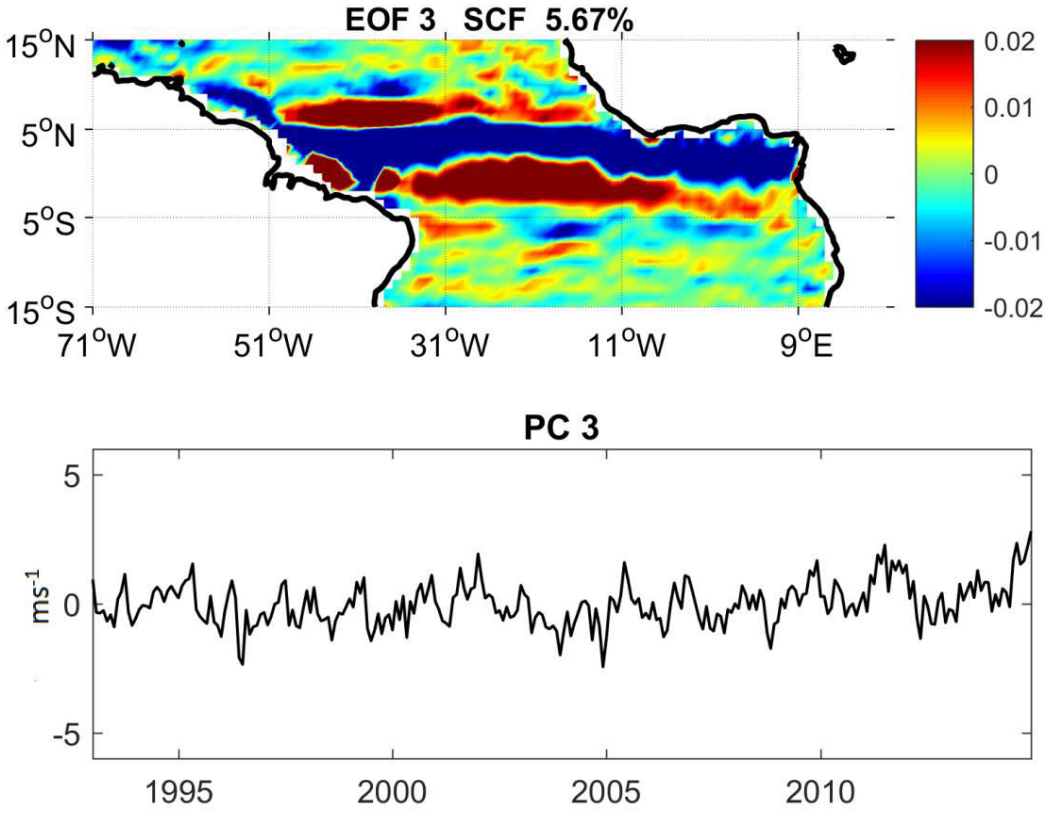

Source: The Author

WAVELET ANALYSIS OF THE ZONAL COMPONENTS

For the zonal component, the wavelet analyses of the PC1 presents the strongest variance signal with 12-month and 6-month period mainly in 2004-2005 and 2008-2009 (Figure 11). The years 2004-2005 were marked by the negative phase of Atlantic Niño,

respectively explain strongest south easterly winds and strong positive zonal currents anomaly. The strong variance identified in 2008 coincides with a strong negative anomaly in the PC1 and a positive phase of Atlantic Niño.

In the PC2, the dominant periodicities of strongest variance are in the annual band, between 1997 and 1999, and for 32-month period from the 1996 to 1999 and a strong interannual signal in the years 2008 to 2011. In PC2 also were identified intraseasonal peaks in the variance in 1998, 2001, 2009 and 2012.

For the wavelet analyses in the PC3, two intraseasonal peaks were showed in 1996 and 2004, one for 16-month period between 2004 and 2007, and another for 24-month period during 2010 and 2011 (Figure 11).

Figure 11 – The wavelet transform of the Principal Components (PC1, PC2 and PC3) from the EOF1, EOF2 and EOF3 respectively of the zonal component along the Tropical Atlantic.

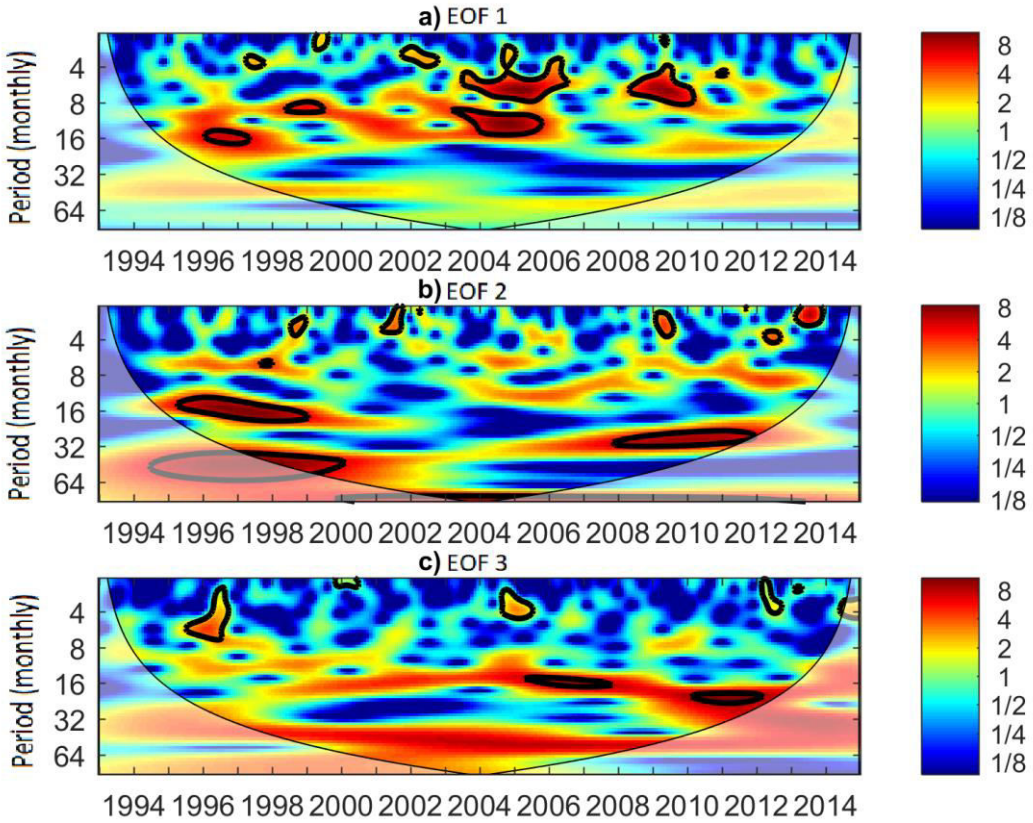

Source: The Author

EOF ANALYSIS OF THE SURFACE CURRENT VELOCITIES

The next results show the EOF of the current speed (Figures 12, 13, 14), which explain about 43% of the total variance. The EOF1 of current speed (~ 30.0%) shows a dominant negative signal covering a broad area between 5ºS-5ºN and crossing the Atlantic basin (Figure 12). This signal is related with the cCSE, which flows towards the west. In contrast, a positive and weak signal at 7° N exists but it is not well defined as a pattern of current.

Figure 12 – First EOF mode of 24 years of the surface current speed, the SCF in percentage, and the PC1.

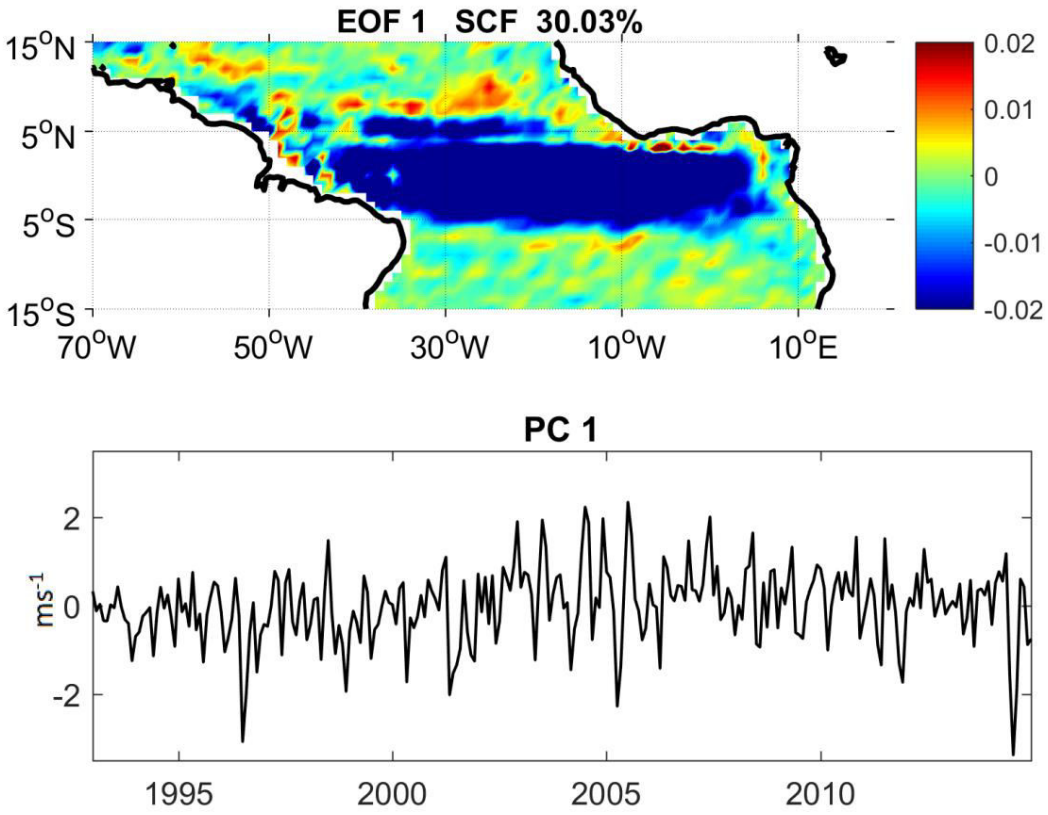

Source: The Author

The EOF2 retains 8.16% (Figure 13) of the total variance. This mode highlights the zonal dipole in the equatorial region, as detected in the second mode of the zonal currents. The negative signal covers the region of the cold tongue in the eastern equatorial Atlantic (CANIAUX *et al.*, 2011), which is controlled by BF.

In contrast, on the western of the TA, the positive signal covers the warm pool region, and to the north a positive signal is associated with NBC retroflection feeding the NECC.

The EOF3 represents 5.60% of total variance, (Figure 14) of the total variance. The spatial pattern in the western TA shows high variability, with alternating signals of positive and negative values, however it is not a well-defined pattern. In the eastern TA there are well-defined structures of alternating signals of negative and positive anomalies, between 5ºS at 5ºN. (Figure 14).

Figure 13 – Second EOF mode of 24 years of the surface current speed, the SCF in percentage, and the PC2.

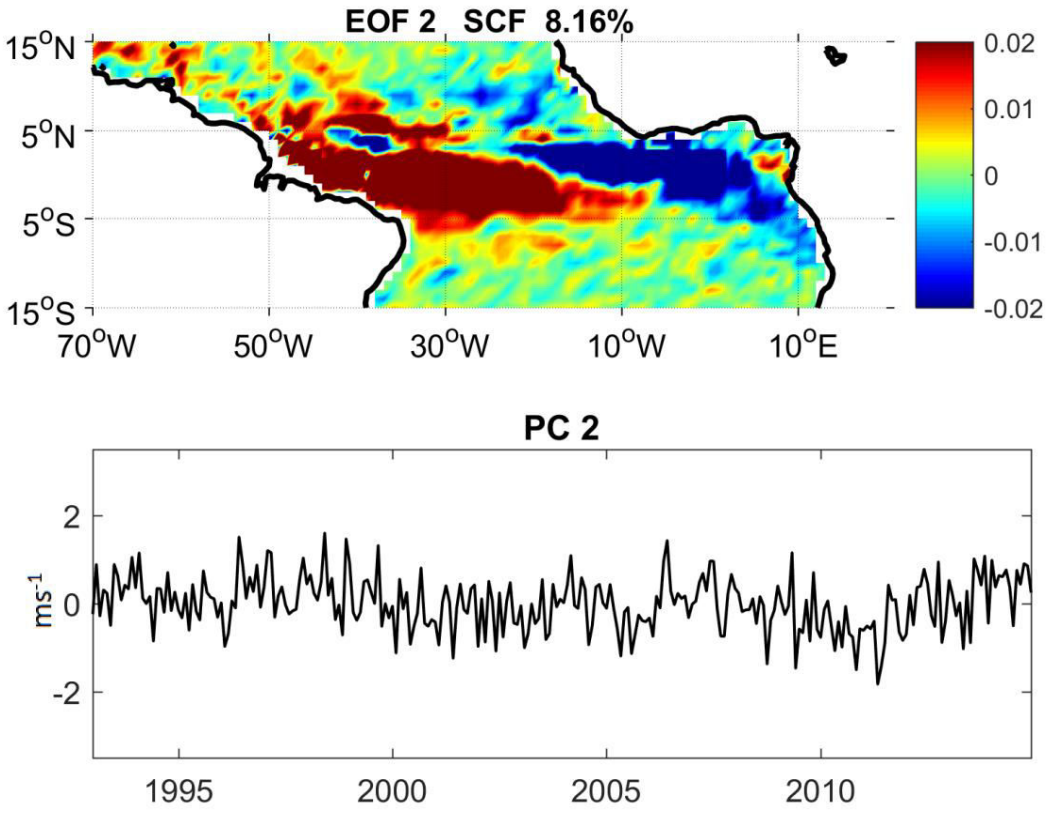

Source: The Author

The EOF3 represents 5.60% of total variance, (Figure 14) of the total variance. The spatial pattern in the western TA shows high variability, with alternating signals of positive and negative values, however it is not a well-defined pattern. In the eastern TA there are well-defined structures of alternating signals of negative and positive anomalies, between 5ºS at 5ºN. (Figure 14).

Figure 14 – Third EOF mode of 24 years of the surface current speed, the SCF in percentage, and the PC3.

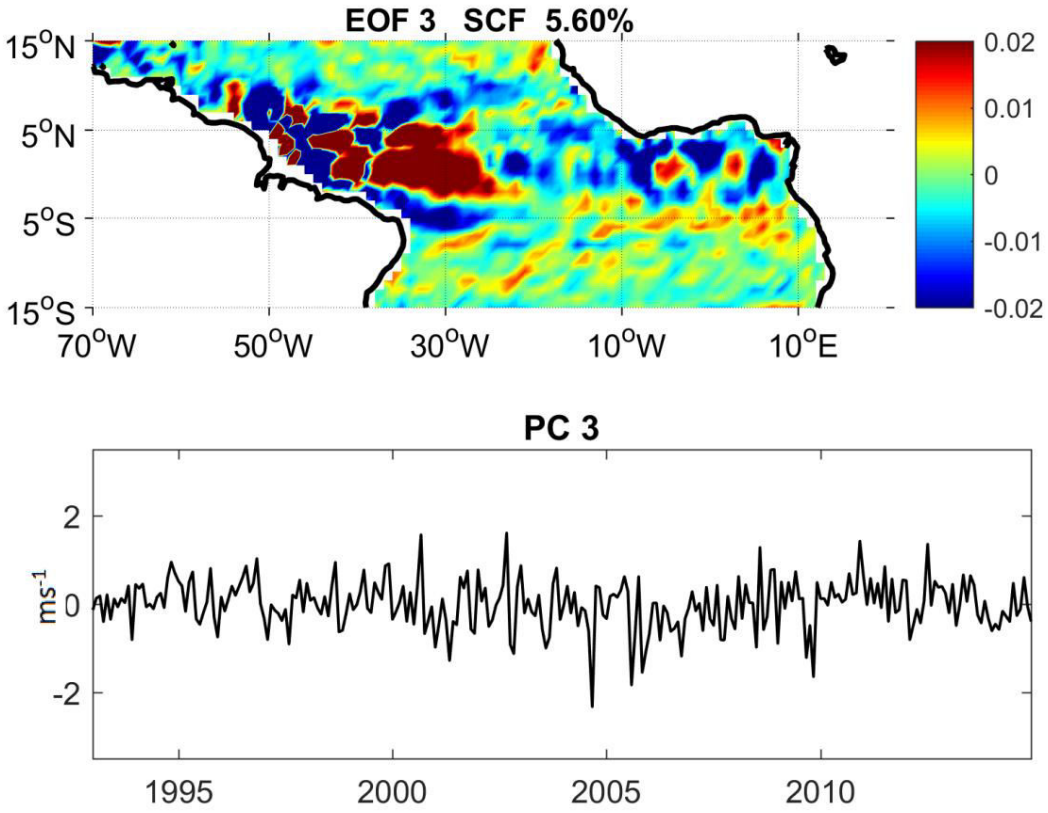

Source: The Author

WAVELET ANALYSIS OF THE SURFACE CURRENT VELOCITIES

Since the PCs showed similar pattern with high frequency oscillations, wavelet analyses were performed for the PCs of each mode of surface currents (Figure 15). The PC1 wavelet analyses showed the stronger variance mainly between 2004 and 2005 with about 6-

months periodicity. The negative phase of the Atlantic Niño present in 2004-2005 could explain the strong variance in the surface current velocities in these years, as identified in the PC1 of the zonal components. The PC2 showed a peak for 36-month period between 2004 and 2005. The PC3 showed three dominant periodicities of strong variance, the first was between 1996 and 1997 for 16-month period, the second was during the 2004 and 2005 with 16-month periodicity, and the third for the 24-month period between 2010 and 2011.

Figure 15 – The wavelet transform of the Principal Components (PC1, PC2 and PC3) from the EOF1, EOF2 and EOF3 respectively of the surface current speed along the Tropical Atlantic.

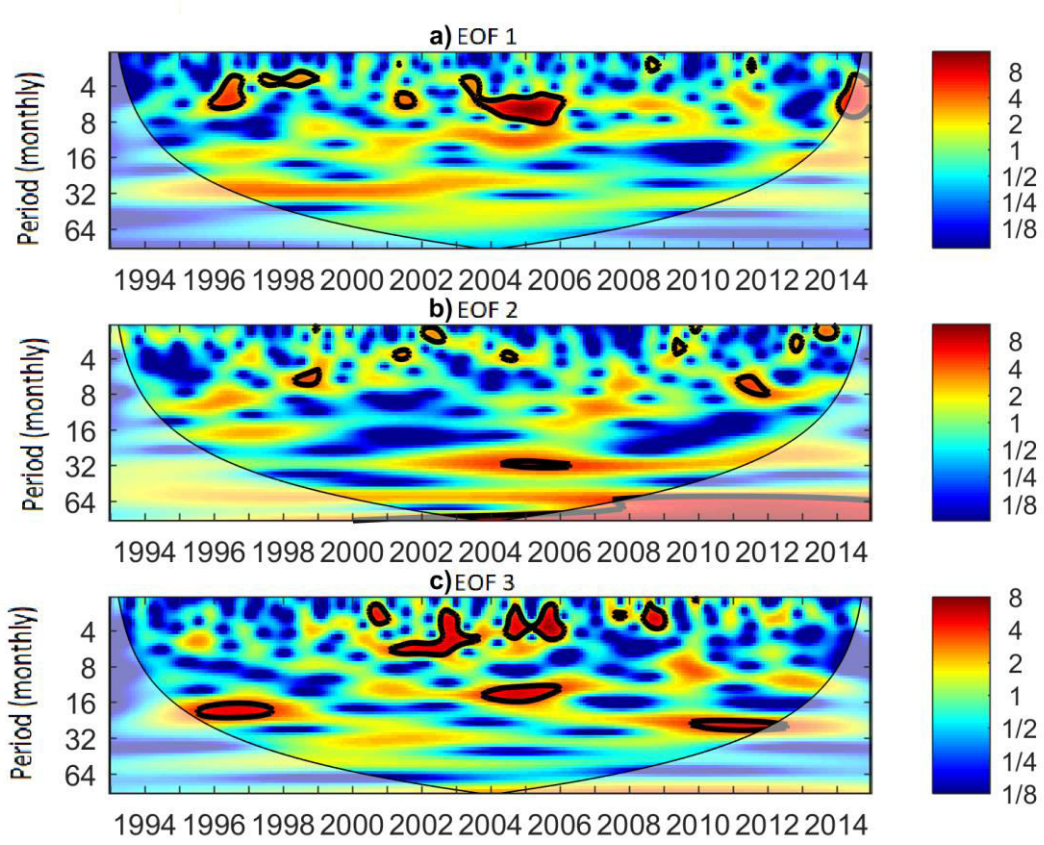

Source: The Author

4.2 SPATIAL AND TEMPORAL VARIABILITY OF CHLOROPHYLL *a* CONCENTRATION IN TROPICAL ATLANTIC USING EMPIRICAL ORTHOGONAL FUNCTION ANALYSIS OF SATELLITE IMAGES

In this section are presented the main modes of Chl concentration variability, identified through the EOF analysis. The EOF of Chl was applied to the domain of 20°S to 20°N in the TA. Despite the Chl spatial resolution to be 4km, in this analysis it was applied to 1/2 degree in order to reduce computational efforts. The EOF modes and their respective PCs were performed to the Chl (mg m^{-3}) anomaly in log_{10} scale. The analysed results allowed quantifying the main variability modes of Chl in the TA.

The Figure 16 shows the main patterns identified in the Chl concentration. In the EOF1, the spatial pattern explained 15.36% of the total variance (Figure 16). The main characteristic of the first mode shows two dominant positive signals in the spatial pattern. One of these dominant positive signals is confined to the WTNA, covering the area between 18°N – 5°S and 60°W- 55°W. This high variance of Chl is associated with the Amazon River plume position, once the discharge of continental waters rich in nutrients are transported through the NBC northwestward, between 50°W-60°W (SILVA *et al*., 2009). The WTNA is also characterized as a particularly high-energy marine system by the NBC retroflection and rings variability (JOHNS *et al.,* 1998). Besides that, at the 7° N, the EOF1 shows a weaker positive signal from approximately 51° W to 30° W (Figure 16), covering the region of the NECC position. This signal is associated with the NECC, which carries eastward the Amazon plume nutrients during the austral spring through fall (FRATANTONI and GLICKSON, 2002).

Further northeast, a dominant positive anomaly occurs between 20°N- 10°N and about 28°W – 7ºW along the northwest African coast, covering the Senegalo-Mauritanian upwelling region (Figure 16). In this case, according to Capet *et al.* (2017) the wind regime is responsible for the coastal upwelling between the Cape Verde Archipelago (~18°N) and Cape Roxo (~12°N). Conversely, a weak positive signal covers the region of the ACT and crossing the TA along the equator (10°E - 30°W) from 2°N to 10°S (Figure 16). However, Jouanno (2011) identified the main peak of Chl concentration from 20°W to 10°W and between 18°S and equator in June-August. This signal may be weak due the high cloud cover in the equatorial band. Additionally, the equatorial upwelling also increase the Chl concentration in

this region by the nutrient flux into the mixed layer from the subsurface waters. Nutrient supply is a limiting factor for photosynthesis, since the solar radiation has abundant availability along the equator (LONGHURST, 1993). Thus, it was expected a dominant positive signal occur in the region that covers the ACT and equatorial upwelling (Figure 16). The temporal amplitude of this mode exhibited positive intraseasonal peaks in the late of 2004, 2009, 2010, 2011 and 2016 (Figure 16).

Figure 16 – The first EOF mode for Chl anomaly using Aqua-MODIS Chl (mg m^{-3}) in log_{10} scale, during 2003–2016 in the TA, the SCF in percentage, and the PC1.

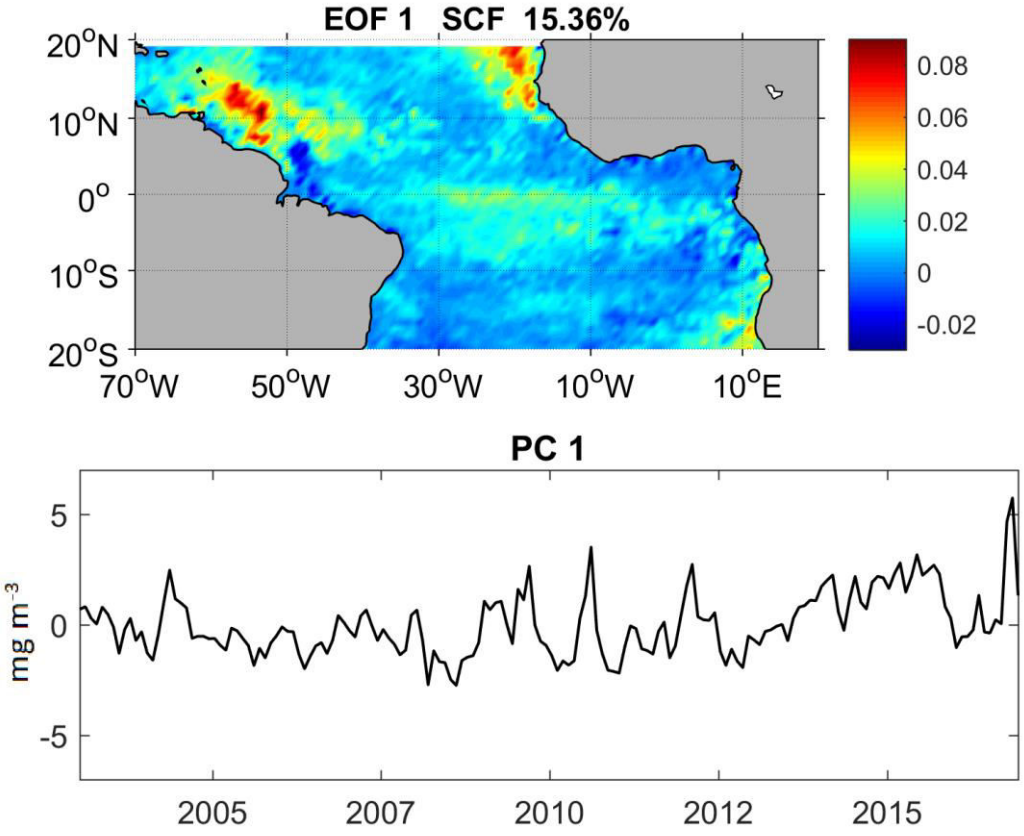

Source: The Author

The spatial pattern of EOF2 of Chl concentration (Figure 17) corresponded to 9.45% of the total covariance. As in the EOF1, the main characteristic of the second mode shows a spatial pattern of dominant positive signal, also confined to the WTNA. In contrast, in the EOF2 I identify a westward shift of this signal (between 55°W to 65°W). Further south, at

7°N a weak positive sign extends eastward, which can be associated with a transport of Amazon plume by the NECC.

Another weak positive signal of Chl is in approximately 8°S, near to the Congo River discharge. Besides that, another centre of Chl anomalies was located in an area with the geographical coordinates of about 13°S - 20°S at 10°E (Figure 17). In this case, the positive signal occurs along shore of the Benguela upwelling. According to Liu and Wang (2013) the Benguela upwelling region is affected mainly by the stronger mixing of the water column bringing deeper nutrients upward, in turn favouring a phytoplankton bloom.

The PC of EOF2 showed that a maximum of Chl anomaly occurred in 2010 and the minimum Chl was observed in 2005 (Figure 17).

Figure 17 –**.** The second EOF mode for Chl anomaly using Aqua-MODIS Chl (mg m^{-3}) in log_{10} scale, during 2003–2016 in the TA, the SCF in percentage, and the PC2.

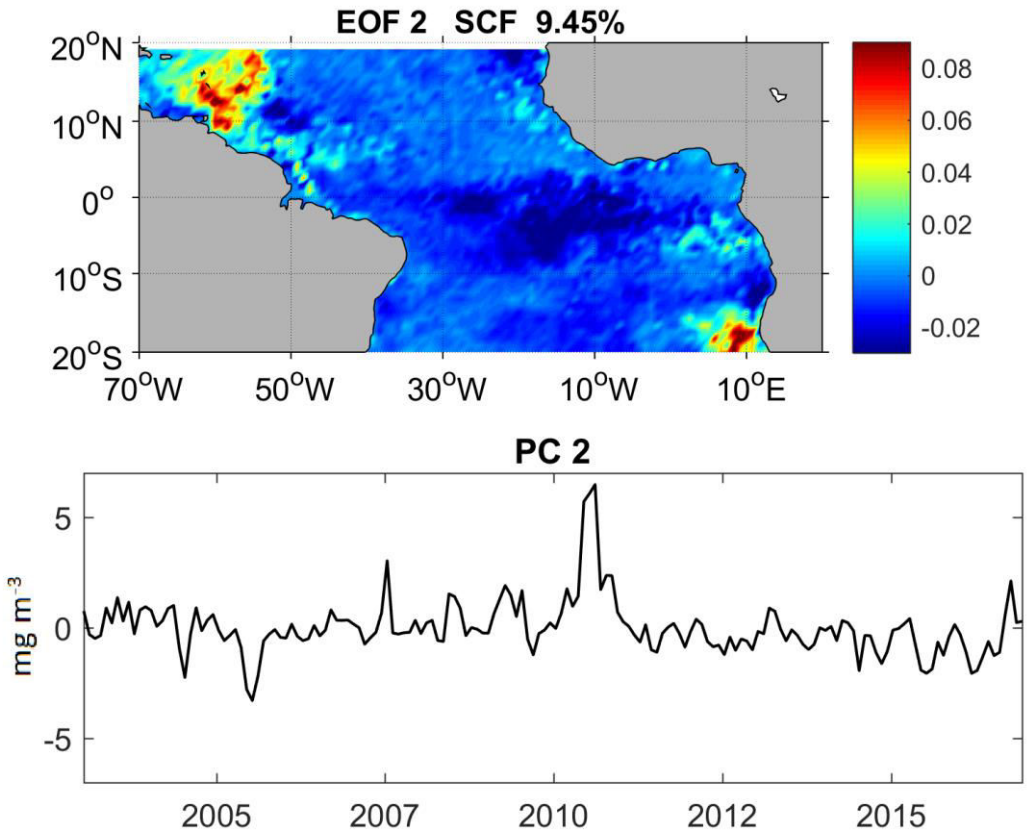

Source: The Author

The EOF3 retains 7.20% (Figure 18) of the total covariance, showing a dominant positive signal similar which was found in EOF1, covering the area between 7ºS at 12ºN and 40ºW at 35ºW (Figure 18). The third mode shows a similar pattern to the EOF1, but weaker positive signal near the African coast (10°E- 30°E), confined between 8°S to 1°N (Figure 18). Thereby, I identified that this region covers the ACT and equatorial divergence, which is associated with the highest Chl concentrations from 20°W to 10°W and between 1°S and equator (JOUANNO, 2011). Furthermore, according to Jouanno (2011) at 4°S and 5°E a maximum pattern of Chl is associated with the Congo River plume and coastal upwelling (SIGNORINI *et al*., 1999).

The PC of EOF3 showed a pattern with high frequency oscillations in comparing on EOF1 and EOF3. The PC3 showed three dominant periodicities of strong variance, the periods between the years of 2007-2008, 2009-2010 and 2016 (Figure 18).

Figure 18 – The third EOF mode for Chl anomaly using Aqua-MODIS Chl (mg m^{-3}) in log_{10} scale, during 2003–2016 in the TA, the SCF in percentage, and the PC3.

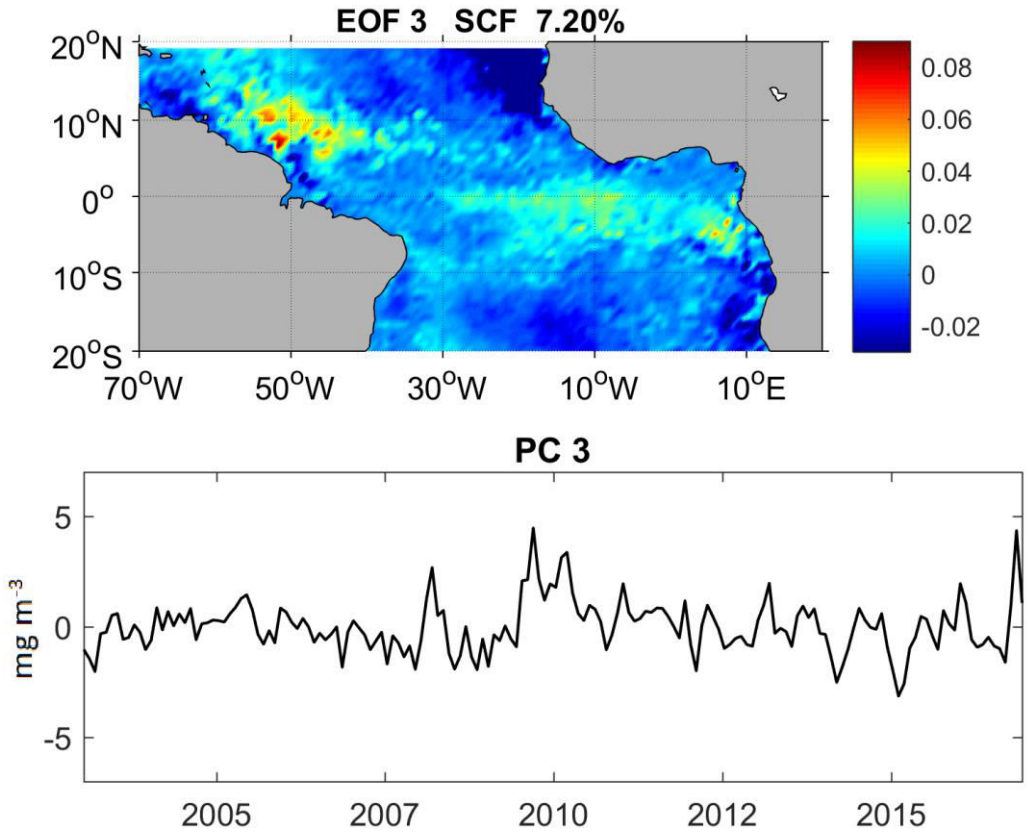

Source: The Author

The EOF4 represents 4.85% (Figure 19) of the total variance. The spatial pattern in the western TA shows high variability with positive signal from 60°W to 30°W at 10°N. A dominant centre of Chl is confined between 50°W and 45°W, which covers the NBC retroflection area (Figure 19). According to Bourlès *et al.* (1999), the NBC expands and retroflects eastward between 5°N and 10°N during the predominant period of the Southeast trade winds. Seasonally, the NBC retroflection carries waters from the Amazon River plume and feeds the NECC (RICHARDSON and REVERDIN, 1987; FONSECA *et al.,* 2004; COLES *et al.,* 2013). Consequently, it causes a bloom in the middle of the TA basin. The PC of the EOF4 exhibited a dominant positive intraseasonal peak in 2016 (Figure 19).

Figure 19 – The fourth EOF mode for Chl anomaly using Aqua-MODIS Chl (mg m^{-3}) in log_{10} scale, during 2003–2016 in the TA, the SCF in percentage, and the PC4.

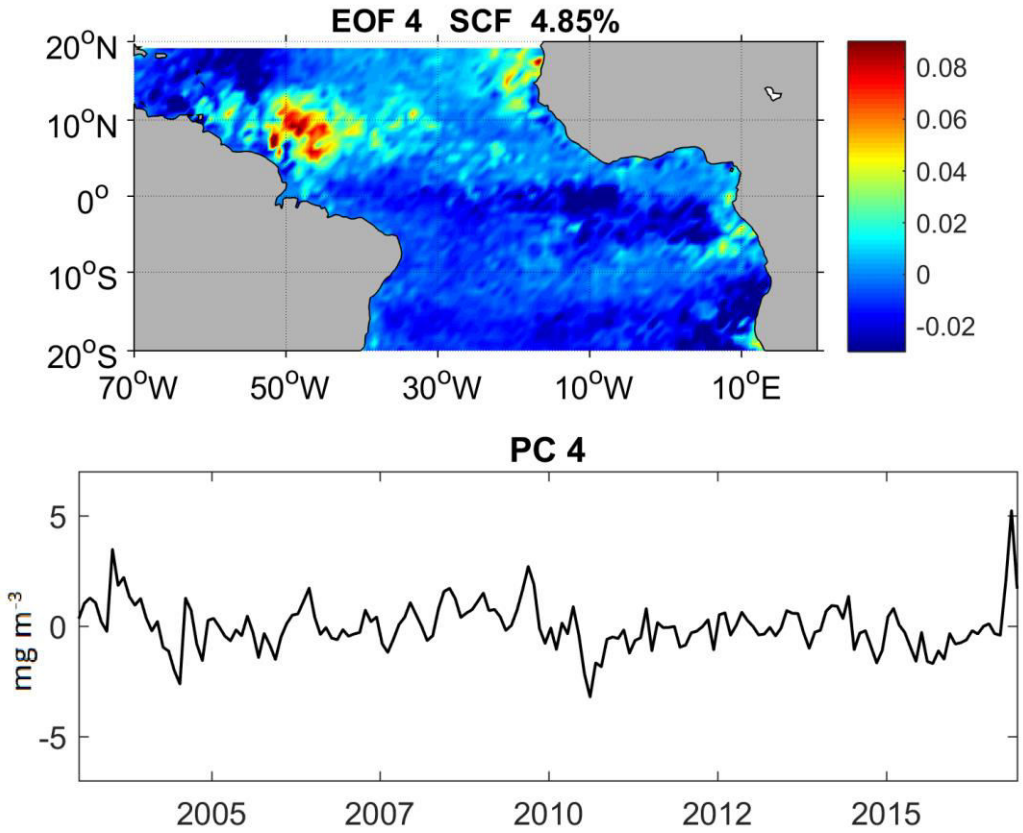

Source: The Author

4.3 COUPLED EOF BETWEEN SURFACE CURRENTS AND CHLOROPHYLL *a*

In this section are presented the main coupled modes of variability between surface currents and Chl concentration, identified through the EOF analysis. In order to reduce computational efforts, the both surface ocean currents and Chl data were used with a spatial resolution of 1 degree in the TA. The time period used in this analysis was between 2003 and 2017. The EOF analysis of the cross-covariance matrix between surface currents and *Chl* revealed three main modes. The first three modes explained 42.08% of the total covariance between surface currents and Chl, with 25.22, 9.92 and 6.24% of the signal explained by EOF1, EOF2, and EOF3 respectively.

The first mode (EOF1) explained 25.22% of the covariance (Figure 20) and the PC1 surface current signal was correlated with Chl. The main characteristic of the first mode is a spatial pattern with positive anomalies of currents and Chl over the equatorial Atlantic and Amazon plume region.

EOF1 presented positive surface current anomalies, covering the area between 10ºS and 10ºN and 35ºW and 10ºE (Figure 20).This pattern is associated with an east-west axis of positive Chl anomalies over the equatorial Atlantic. Thereby, the surface currents were positively correlated with Chl concentration, covering the cSEC flow and the divergence equatorial area. The equatorial divergence variability is linked with larger-scale climate variability by tropical ocean–atmosphere feedbacks (SARAVANAN and CHANG, 2004), and with longer-time-scale global variability through the Atlantic Meridional Overturning Circulation (AMOC). Besides that, equatorial divergence is globally important since the upwelling is strong and primary productivity is high where wind-driven surface currents diverge (CHAVEZ and BARBER, 1987; VOITURIEZ and HERBLAND, 1981).

Moreover, the corresponding EOF1 spatial pattern of surface current near the Brazilian coast shows also positive anomalies from 35°W to 50ºW, along the NBC flow and Amazon plume area (Figure 20).This pattern is associated with a northwestward axis (50°W) of positive Chl anomalies, covering the Amazon plume. Similar structures were also detected by Molleri *et al*. 2010, who identified the first dispersion pattern at the Amazon plume flowing to northwest along the South American coast, from January to April, by the NBC.

Figure 20 – First coupled EOF mode of covariance matrix between surface current and *Chl* (mg m^{-3}) in log_{10} scale, the SCF in percentage, and the PC1.

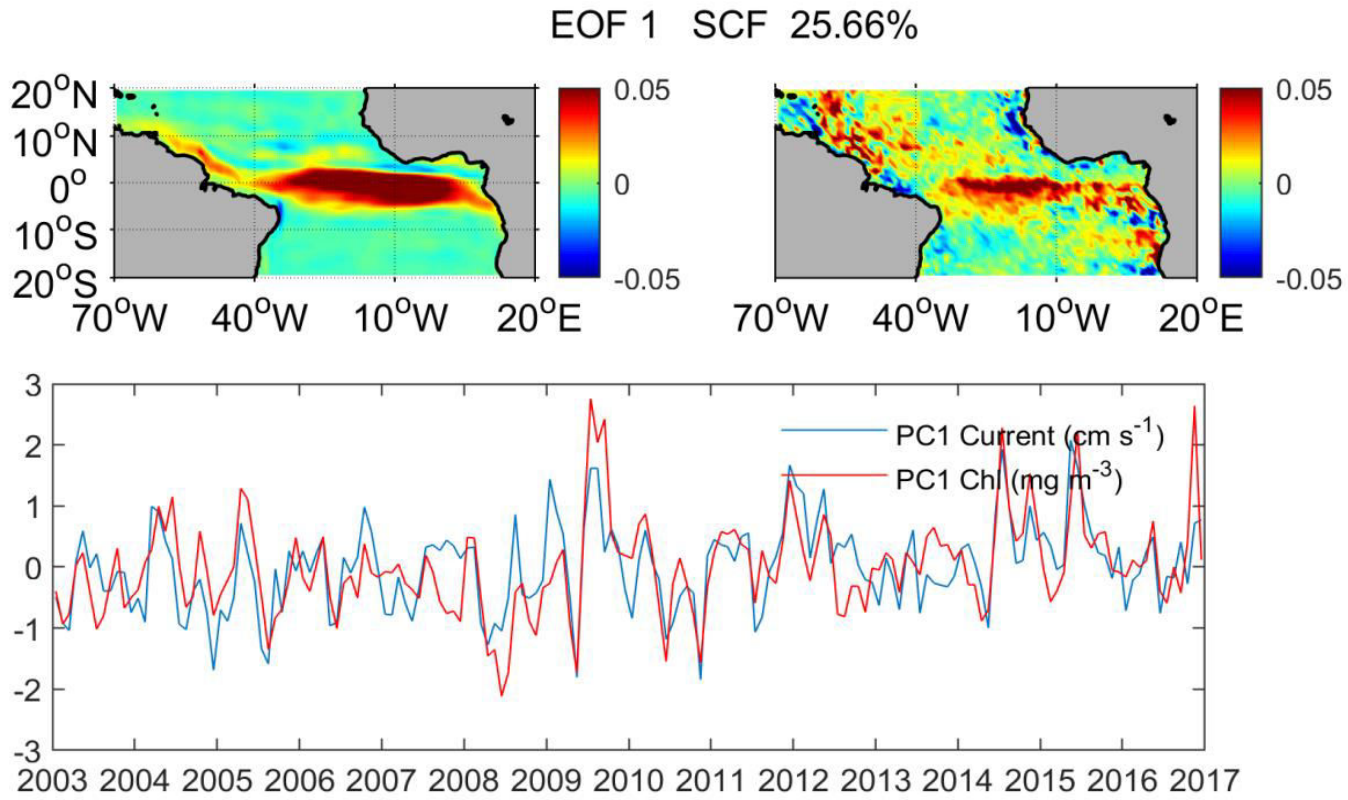

Source: The Author

The PC1 of both surface currents and Chl are positively correlated (0.8) and in phase, evidencing that in the EOF1, when the currents intensify the Chl concentration is higher.

The EOF2 (Figure 21) explained 9.92% of the covariance. The main spatial pattern of surface currents shows negative anomaly along the equator, delimited by two positives axis, one to the north and another to the south. This spatial pattern is associated to the positive anomaly, restrict to the east of the basin, south of equator, between 10°W and 20°E, of the main Chl spatial pattern, covering the region of the ACT near the African coast. These patterns are associated with the ACT variability, which develops rapidly when the cross-equatorial southerlies intensify and reaches its peak in July–August (OKUMURA and XIE, 2004). From September onward, the ACT is reduced by the southerly cross–equatorial winds

weakening (DEPPENMEIER *et al.*, 2016). Consequently, the seasonal main peak of Chl concentration is during the period from June to August from 20°W to 10°W (JOUANNO, 2011). Furthermore, the EOF2 showed a dominant positive anomaly for Chl from the Amazon mouth in the WTNA, and a weak signal of positive anomaly in the retroflection centred at 50°W and an eastward propagation along 6–8°N.

Figure 21 – Second coupled EOF mode of covariance matrix between surface current and *Chl* (mg m^{-3}) in log_{10} scale, the SCF in percentage, and the PC2.

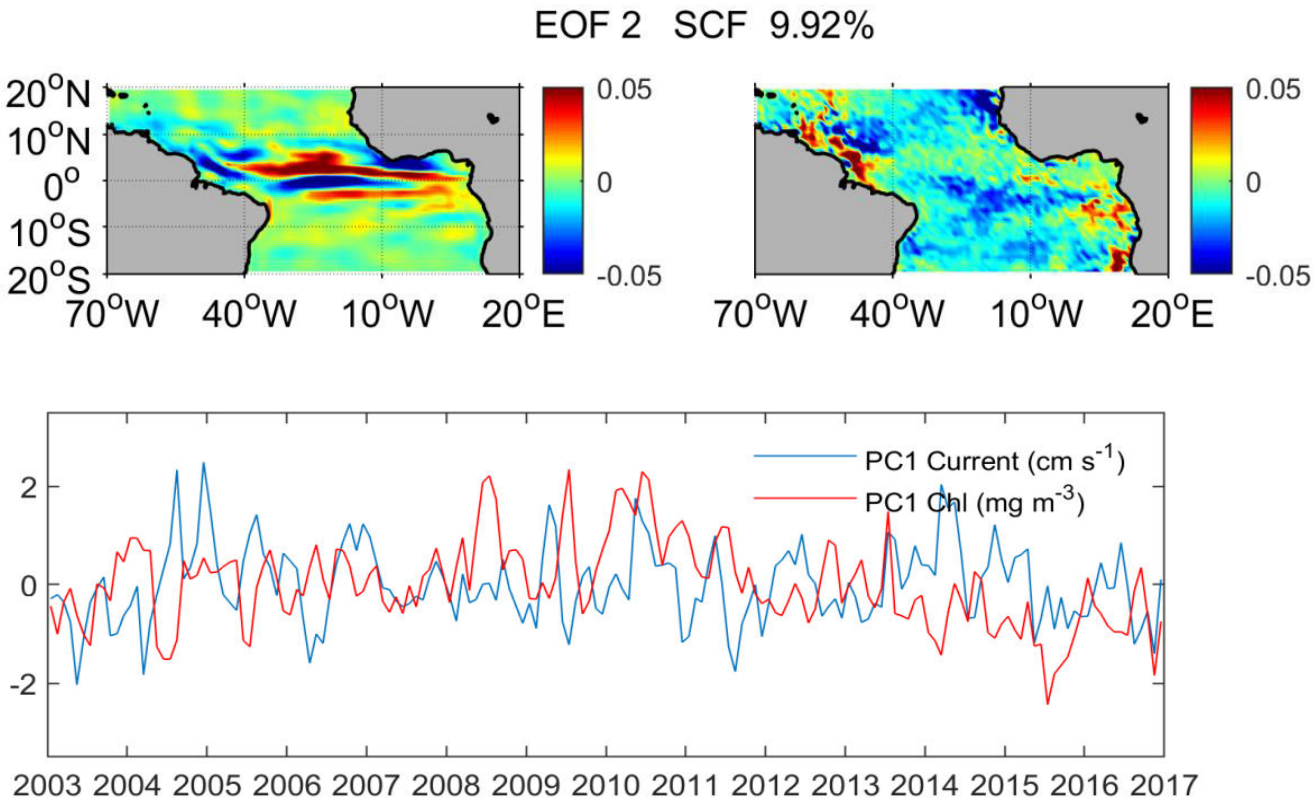

Source: The Author

The PC2 of the surface currents are opposite to the Chl, highlighting the negative response of the Chl to the surface currents in the EOF2. The EOF patterns confirm in the region of the NBC that exists a negative signal in currents associated to a positive signal in the Chl pattern. Also, positive signals of the currents in the middle of south Atlantic are associated to negative Chl anomalies.

The spatial pattern of EOF3 (Figure 22) retains about 6% of the covariance and exhibited the surface current structure similar to the EOF2 (Figure 21). However, the EOF3 shows a dominant positive anomaly of surface current in the Congo plume region. This pattern is associated with positive anomaly of Chl in the spatial pattern covering the Congo River discharge. According to Hopkins *et al*. (2013), the Congo plume extends between 400 and 1000 km northwest or west–southwest out into the open south Atlantic. This Congo plume variability is associated with the current intensity and direction, such as the Angola and Benguela Coastal currents.

Further south of the equator, at east (between 30°W and 10°E), a positive Chl anomaly pattern is found. This pattern can be associated with the ACT variability when the ITCZ migrates southward, from March to April in around 5°S (GEYER *et al.*, 1996).

Figure 22 – Third coupled EOF mode of covariance matrix between surface current and *Chl* (mg m^{-3}) in log_{10} scale, the SCF in percentage, and the PC3.

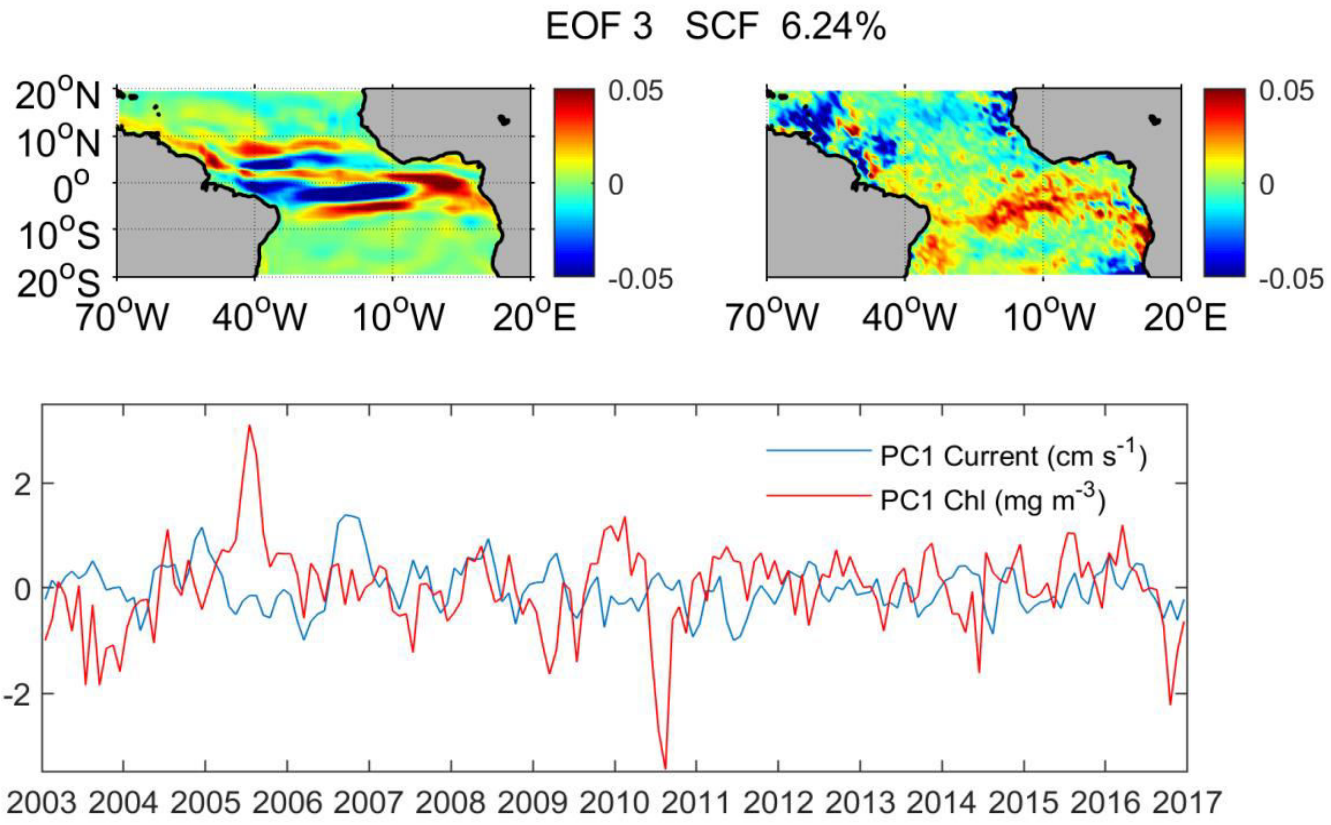

Source: The Author

The PC3 shows that the most time the Chl is responding positively to the surface currents, with exception of 2005 and 2010, when strong anomalies are detected in the Chl.

5 CONCLUSIONS

This work aims to contribute to a better understanding of the surface circulation dynamics and Chl concentration in the TA. Specifically, the main objective of this work is to analyse the Chl concentration response to the surface currents variability in the TA. Three analyses were performed using monthly data. The EOF of surface circulation, with 24 years and the EOF of Chl with 14 years. In the last analysis of the coupled EOF between surface currents and Chl, I used 15 years of both variables, once the database of Chl was actualized to more recent years.

In the surface current speed analysis, I can infer the dominant role of the zonal component in the TA. EOF1of surface currents speed (~30%) showed a dominant negative signal covering a large area crossing the Atlantic basin, related to the cCSE which flows westward. The EOF2 (8.16%) showed the importance of the zonal dipole, similar in the spatial pattern and variance to the zonal EOF2 (8.23%) of the zonal component. This pattern in the western of TA covers the area of the Warm Pool and the cold tongue area at the eastern of the TA. Thus, the large-scale surface circulation in the TA is characterized by strong zonal variability and this upper-ocean zonal current system, which is very important for the interhemispheric and west-to-east exchange of heat and nutrients.

At the equatorial region, the wind-driven surface currents divergence increases the primary productivity and Chl is carried by cSEC along the equatorial Atlantic. Close to the American shelf, the NBC carries Chl from the Amazon plume water, rich in nutrients, northwestwards, arriving at the Caribbean and the Central Equatorial Atlantic Ocean (HELLWEGER and GORDON, 2002).

In the east of the TA, the high variance of Chl is associated with ACT variability that develops by cross-equatorial southerlies intensification. In the Congo plume region, to the west of the basin, a positive variance of Chl is associated with a positive variance of surface currents. This result corroborates with Hopkins *et al*., 2013, who has identified that the Congo plume extends between 400 and 1000 km northwest or west–southwest to the open ocean.

The main results of this work are the coupled modes presented in section 4.3, which provide the co-variability between surface currents and Chl over the TA, which revealed three main coupled modes that explained 42.08% of the total covariance.

The coupled first EOF between surface currents and Chl evidence the main patterns of positive anomalies as the equatorial divergence and the Amazon plume dispersion, representing about 25% of covariance. The PCs for each variable are positively correlated and in phase, evidencing that this pattern of Chl can be monitored by the patterns of currents in the TA.

The second coupled EOF that retains about 9% of covariance is characterized by an axis of negative anomalies in the equatorial region, followed by positive anomalies at north and south. This pattern is associated to a low Chl distribution in the center of the basin and the Chl positive anomalies are restrict to the Congo plume region, at east.

The third coupled EOF pattern presents a similar spatial pattern as in the EOF2, however this pattern of positive and negative anomalies axes is shifted to the south. In this pattern is possible to identify that the positive current pattern anomaly, at south of equator, is strong and extends from the African coast, crossing the basin to the west. This pattern is associated to a distribution of Chl that also extends from the African coast to near the Brazilian coast.

Despite this pattern represents a low covariance between currents and Chl, about 6% of covariance, when this pattern occurs it is favourable to an increase of Chl in the whole basin.

Knowledge of the heterogeneity of Chl concentration and surface circulation in oligotrophic waters is essential for understanding the dynamics of marine ecosystems. As the main optical variable, Chl plays an important role in biogeochemistry of phytoplankton photosynthesis. Besides that, the ocean surface circulation plays an important role in climate dynamics, thermohaline circulation, mass and heat distribution and also reflects the patterns of ocean-atmosphere fluxes, evaporation and precipitation, heat and energy.

6 PERSPECTIVES

This study can contribute for coupled modes analysis of Chl and altimetry of the Tropical Atlantic. The first results were published in a scientific journal, and these last results are still in process and discussion, to be published as a scientific manuscript.

Moreover, this study has the potential base line for further investigations, associated to large-scale climatic variability, circulation dynamics, air-sea heat fluxes once the light absorption by chlorophyll leads to the modification of the penetrating heating flux in the water column, CO_2 uptake as the primary production is an important sink of CO_2 and ecological impacts on the food chain, once phytoplankton is food for other plankton and small fish, as well as larger animals. The knowledge of the ocean dynamics is necessary for understanding the effects that control the interannual climatic variability and interactions between tropics and subtropics (SCHOUTEN et al., 2005).

Besides that, this work also contributes to the further research on biogeochemical cycles in the TA once phytoplankton plays a crucial biogeochemical role, converting CO_2 and nutrients into particulate organic and inorganic matter via photosynthesis and biomineralization, respectively (DONEY *et al*., 2010). Thereby, the photosynthesis process is determinant in the carbon cycle due to they regulate the carbon export to the sediments (SARMIENTO and GRUBER, 2006).

Therefore, the results of this work contribute to the understanding of the surface currents dynamics, zonal and meridional transport variability of Chl concentration, and ocean-atmosphere interaction processes. Thus, this study allows predicting the dispersion of Chl by the surface currents in the TA.

REFERENCES

ACKER, J.; WILLIAMS R.; CHIU, L; ANDANUY, P.; MILLER, S.; SCHUELER, C.; VACHON, P. W.; MANORE, M. Remote Sensing from Satellites. In: MEYERS, Robert A.(Ed.) **Encyclopedia of Physical Science and Technology**, 3. ed. New York: Elsevier, p.161-202, 2003, doi:10.1016/B978-0-12-409548-9.09440-9.

ARNAULT, S. AND KESTENARE, E. Tropical Atlantic surface current variability from 10 years of TOPEX/Poséïdon altimetry, **Geophysical Research Letters**, v. 31, L03308. p. 1-4, 2004, doi:10.1029/2003GL019210.

BJERKNES, J., Atmospheric Teleconnections From The Equatorial Pacific. **Monthly Weather Review**, 97, 163–172, 1969, doi:10.1175/1520-0493(1969)097<0163:ATFTEP>2.3.CO;2.

BAKUN, A. Guinea Current upwelling, **Nature**, v. 271, p. 147–150, 1978.doi: 10.1038/271147a0.

BEHRENFELD M J AND FALKOWSKI P G. Photosynthetic rates derived from satellite based chlorophyll concentration, **Limnology Oceanography**. 42 1–20, 1997, doi: 10.4319/lo.1983.28.2.0320.

BONJEAN, F. AND LAGERLOEF, G. S. Diagnostic Model and Analysis of the Surface Currents in the Tropical Pacific Ocean, **Journal of Physical Oceanography**, v. 32, p. 2938–2954, 2002, doi: 10.1175/1520-0485(2002)032<2938:DMAAOT>2.0.CO;2.

BOURLÈS, B.; GOURIOU, Y. AND CHUCHLA, R. On the circulation in the upper layer of the western equatorial Atlantic, **Journal of Geophysical Research**, v. 104, issueC9, p. 21151–21170, 1999, doi: 10.1029/1999JC900058.

BRANDT, P.; HORMANN, V.; BOURLÈS, B.; FISCHER, J.; SCHOTT, F.A.; STRAMMA, L. AND DENGLER, M. Oxygen tongues and zonal currents in the equatorial Atlantic, **Journal of Geophysical Research**, v. 113, C04012, p. 1-15, 2008, doi:10.1029/2007JC004435.

BRANDT, P. *et al*., Circulation in the central equatorial Atlantic: Mean and intraseasonal to seasonal variability. **Geophysical Research Letters,** 33, L07609, 2006, doi:10.1029/2005GL025498.

CANIAUX, G., GIORDANI, H.; REDELSPERGER, J. L.; GUICHARD, F.; KEY, E. AND WADE, M. Coupling between the Atlantic cold tongue and the West African monsoon in boreal spring and summer, **Journal of Geophysical Research**, v. 116, C04003, p. 1-17, 2011,doi: 10.1029/2010JC006570.

CAPET, X., P. ESTRADE, E. MACHU, S. NDOYE, J. GRELET, A. LAZAR, L. MARIÉ, D. DAUSSE, AND P. BREHMER, On the Dynamics of the Southern Senegal Upwelling Center: Observed Variability from Synoptic to Superinertial Scales. **Journal of Physical Oceanography,** 47, 155–180, 2017, doi: 10.1175/JPO-D-15-0247.1.

CHANG, P., R. SARAVANAN, T. DELSOLE, F. WANG, Predictability of Linear Coupled Systems. **Part I:Theory, Journal of Climate**, 17, 1474-1486, 2004.

CHANG, P.; ZHANG, R.; HZELEGER, W.; WEN, C.; WAN, X., LINK, J.; HAARSMA, R.J.; BREUGEM, W.P. AND SEIDEL, H. Oceanic link between abrupt changes in the North Atlantic Ocean and the African monsoon, **Nature Geoscience**, v. 1, p. 444–448, 2008, doi: 10.1038/ngeo218.

CHAVEZ, F.P., MESSIÉ, M., A comparison of eastern boundary upwelling ecosystems. **Progress in Oceanography, .**83, 80–96, 200, doi:10.1016/j.pocean.2009.07.032.

CHISHOLM, S. W., AND F. M. M. MOREL, What controls phytoplankton production in nutrient-rich areas of the open sea?,**Limnology Oceanography**, 535 36, 1507–1970, 1991.

COLES, V.J.; BROOKS, M.T.; HOPKINS, J.; STUKEL, M.R.; YAGER, P.L.; AND HOOD, R. R. The pathways and properties of the Amazon River plume in the tropical North Atlantic Ocean, **Journal of Geophysical Research**, v. 118, p. 6894–6913, 2013. doi: 10.1002/2013JC008981.

COX, M.D. Generation and Propagation of 30-Day Waves in a Numerical Model of the Pacific, **Journal of Physical Oceanography**, v. 10, p. 1168–1186, 1980, doi:10.1175/1520-0485(1980)010<1168:GAPODW>2.0.CO;2.

CULLEN, J.J., The Deep Chlorophyll Maximum: Comparing Vertical Profiles of Chlorophyll *a*. Can. J. Fish. Aquat. **Science**. 39, 791–803, 1982, doi: 10.1139/f82-108.

DAUBECHIES, I. Ten Lectures on Wavelets. **CBMS/NSF Series in Applied Mathematics**, v. 61, SIAM, 377 p., 1992.

DAUBECHIES, I. The wavelet transform, time-frequency localization and signal analysis. **IEEE Trans. Inf. Theory**, 36, 961–1005, 1999, doi>10.1109/18.57199.

DAGG M, BENNER R, LOHRENZ S, LAWRENCE D., Transformation of dissolved and particulate materials on continental shelves influenced by large rivers: Plume processes, **Continental Shelf Research** 24, 833–858, 2004. doi: 10.1016/j.csr.2004.02.003.

DE ALMEIDA, R.A.F. AND NOBRE, P. On the Atlantic cold tongue mode and the role of the Pacific ENSO, **Ocean Science, Discussion**, v. 9, p. 163-185, 2012. doi: 10.5194/osd-9-163-2012.

DECCO, H.T. DE, REBELO, A., JUNIOR, T., PEZZI, L.P. AND LANDAU, L. Revisiting tropical instability wave variability in the Atlantic Ocean using SODA reanalysis, **Ocean Dynamics**, v. 68, p. 327–345, 2016, doi:10.1007/s10236-017-1128-2.

DENAMIEL, C., BUDGELL, W.P., TOUMI, R., The Congo river plume: impact of the forcing on the far-field and near-field dynamics. **Journal of Geophysical Research,** 118, 964–989, 2013, doi: 10.1002/jgrc.20062.

DEPPENMEIER, A.L., HAARSMA, R. J. AND HAZELEGER, W. The Bjerknes feedback in the tropical Atlantic in CMIP5 models, **Climate Dynamics**, 47: 2691, 2016. doi:10.1007/s00382-016-2992-z.

DIDDEN, N. and SCHOTT, F. Eddies in the North Brazil Current retroflection region observed by Geosat altimetry, **Journal of Geophysical Research**, v. 98, issue C11, p. 20121–20131, 1993. doi: 10.1029/93JC01184.

DOHAN, K., and MAXIMENKO, N. Monitoring ocean currents with satellite sensors, **Oceanography**, v. 23, p. 94–103, 2010, doi: 10.5670/oceanog.2010.08.

DOHAN, K. Ocean surface currents from satellite data, **Journal of Geophysical Research**, v. 122, p. 2647–2651, 2017. doi:10.1002/2017JC012961.

DOI, T., TOZUKA, T., SASAKI, H., MASUMOTO, Y. AND YAMAGATA, T. Seasonal and interannual variations of oceanic conditions in the Angola Dome, **Journal of Physical Oceanography**, v. 37, p. 2698–2713, 2007. doi: 10.1175/2007JPO3552.1.

DONEY, S. C. The growing human footprint on coastal and open-ocean biogeochemistry. **Science** (New York, N.Y.), v. 328, n. 5985, p. 1512–6, 2010. doi:10.1126/science.1185198.

EVANS, W.W., STRUTTON, P.G. AND CHAVEZ, F.P. Impact of tropical instability waves on nutrient and chlorophyll distributions in the equatorial Pacific, **Deep-SeaResearch I,** v. 56, p. 178–188, 2009.

FFIELD, A. North Brazil current rings viewed by TRMM microwave imager SST and the influence of the Amazon plume. **Deep-Sea Research I,** 52, 137–160, 2005. doi: 10.1016/j.dsr.2004.05.013

FLORENZANO, T. G. **Iniciação em sensoriamento remo**to. 3. ed. São Paulo: Oficina de Textos, 2011.

FOLTZ, G. R., GRODSKY, S. A., CARTON, J. A. AND MCPHADEN, M.J. Seasonal mixed layer heat budget of the Tropical Atlantic Ocean, **Journal of Geophysical Research**, Vol. 108 issue C5, 3146, 2003. doi:10.1029/ 2002JC001584.

FONSECA, C.A., GONI, G.J., JOHNS, W.E. AND CAMPOS, E.J.D. Investigation of the North Brazil Current retroflection and North Equatorial Countercurrent variability, **Geophysical Research Letters**, v. 31, L21304, , 2004. doi: 10.1029/2004GL020054.

FRATANTONI, D.M. AND GLICKSON, D.A. North Brazil Current Ring Generation and Evolution Observed with SeaWiFS*, **Journal of Physical Oceanography**, v. 32, p. 1058–1074, 2002. doi: 10.1175/1520-0485(2002)032<1058:NBCRGA>2.0.CO;2.

GANACHAUD, A. AND WUNSCH, C. Improved estimates of global ocean circulation, heat transport and mixing from hydrographic data, **Nature**, v. 408, p. 453–457, 2000. doi:10.1038/35044048.

GARÇON, V. C., A. OSCHLIES, S. C. DONEY, D. MCGILLICUDDY, AND J. WANIEK. The role of mesoscale variability on plankton dynamics in the North Atlantic. **Deep Sea Research Part II Topical Studies in Oceanography**, 2001. 48: 2199–2226, doi:10.1016/S0967-0645(00)00183-1.

GARZOLI, S.L., FFIELD, A., JOHNS, W.E. AND YAO, Q. North Brazil Current retroflection and transports, **Journal of Geophysical Research**, v. 109, C01013, 2004. doi: 10.1029/2003JC001775.

GARZOLI, S.L., FFIELD, A. AND YAO, Q. North Brazil Current rings and the variability in the latitude of the retroflection, in Goni, G.J. and Malanotte-Rizzoli, P. (eds.), Interhemispheric Water Exchange in the Atlantic Ocean, **Elsevier Oceanography Series**, ISBN 0444512675,v. 68, p. 357–373, 2003.

GEYER, W.R., BEARDSLEY, R.C., LENTZ, S.J., CANDELA, J., LIMEBURNER, R., JOHNS, W.E., CASTRO, B.M. AND SOARES, I.D. Physical oceanography of the Amazon shelf, **Continental Shelf Research**, v. 16, p. 575-616, 1996, doi: 10.1016/0278-4343(95)00051-8.

GORDON, A.L. Interocean exchange of thermocline water, **Journal of Geophysical Research**, v. 91, p. 5037–5046, 1986, doi: 10.1029/JC091iC04p05037

HAN, W., WEBSTER, P.J., LIN, J.-L., LIU, W.T., FU, R., YUAN, D. AND HU, A. Dynamics of intraseasonal sea level and thermocline variability in the equatorial Atlantic during 2002-03, **Journal of Physical Oceanography**, v. 38, p. 945–967, 2008, doi:10.1175/2008JPO3854.1.

HARDMAN-MOUNTFORD, N.J., RICHARDSON, A.J., AGENBAG, J.J., HAGEN, E., NYKJAER, L., SHILLINGTON, F.A. ANDVILLACASTIN, C. Ocean climate of the South East Atlantic observed from satellite data and wind models, **Progress in Oceanography**, v. 59, p. 181–221, 2003. doi:10.1016/j.pocean.2003.10.001.

HELLWEGER, F.L., GORDON, A.L., Tracing Amazon River water into the Caribbean Sea. **Journal of Marine Research** 60 (4), 537–549, 2002, doi:10.1357/002224002762324202.

HOPKINS, J., LUCAS, M., DUFAU, C., SUTTON, M., STUM, J., LAURET, O., CHANNELLIERE, C., Detection and variability of the Congo River plume from satellite derived sea surface temperature, salinity ocean colour and sea level. **Remote Sensing of Environment** 139, 365–385, 2013, doi: 10.1016/j.rse.2013.08.015.

HORMANN, V. AND BRANDT, P. Upper equatorial Atlantic variability during 2002 and 2005 associated with equatorial Kelvin waves, **Journal of Geophysical Research**, v. 114, C03007, 2009, doi: 10.1029/2008JC005101.

HORMANN, V., LUMPKIN,R. AND FOLTZ, G.R. Interannual North Equatorial Countercurrent variability and its relation to tropical Atlantic climate modes,**Journal ofGeophysical Research**, v. 117, C04035, 2012. doi: 10.1029/2011JC007697.

HORNING, N. Remote sensing. In: FATH, B. (Ed.) **Encyclopedia of Ecology**. 2. ed. New York: Elsevier, 2018.

HU, C., LEE, Z., & FRANZ, B. Chlorophyll a algorithms for oligotrophic oceans: A novel approach based on three-band reflectance difference. **Journal of Geophysical Research**, 117(C1), 2012, doi: 10.1029/2011jc007395

JOCHUM, M.AND MALANOTTE-RIZZOLI, P. On the generation of North Brazil Current rings, **Journal of Marine Research**, v. 61, p. 147–173, 2003. doi: 10.1357/002224003322005050.

JOHNSON, E.S., BONJEAN, F.,LAGERLOEF, G.S., GUNN, J.T. AND MITCHUM, G.T. Validation and Error Analysis of OSCAR Sea Surface Currents, **Journal of Atmospheric and Oceanic Technology**, v. 24, p. 688–701, 2007, doi: 10.1175/JTECH1971.1.

JOHNS, W.E., LEE, T.N., SCHOTT, F. A., ZANTOPP, R. J. AND EVANS, R.H. The North Brazil Current retroflection: Seasonal structure and eddy variability, **Journal of Geophysical Research**, v. 95, issue C12, p. 22103–22120, 1990, doi: 10.1029/JC095iC12p22103.

JOHNS, W.E., LEE, T.N., BEARDSLEY,R.C., CANDELA,J.,LIMEBURNER, R. AND CASTRO, B. Annual cycle and variability of the North Brazil Current, **Journal of Physical Oceanography**, v. 28, p. 103–128, 1998, doi: 10.1175/1520-0485(1998)028<0103:ACAVOT>2.0.CO;2.

JOUANNO, J., MARIN, F., DU PENHOAT, Y., SHEINBAUM, J. ANDMOLINES, J.M. Seasonal heat balance in the upper 100 m of the equatorial Atlantic Ocean, **Journal of Geophysical Research**, v. 116, C09003, 2011, doi: 10.1029/2010JC006912.

KIRCHNER, K., RHEIN, M., H€UTTL-KABUS, S. AND BÖNING, C. W. On the spreading of South Atlantic Water into the Northern Hemisphere, **Journal of Geophysical Research**, v. 114, C05019, 2009. doi:10.1029/2008JC005165.

KÖRTZINGER, A., A significant CO2 sink in the tropical Atlantic Ocean associated with the Amazon River plume. **Geophysical Research Letters,** 30, 2287, 2003. doi: 10.1029/2003GL018841.

KUMAR, P., AND E. FOUFOULA-GEORGIOU. Wavelet analysis for geophysical applications. **Reviews of Geophysics,** 35, 385–412, 1997, doi: 10.1029/97RG00427.

KWOK, R. Ecology's remote-sensing revolution. **Nature**, v. 556, n. 7699, p. 137-138, 2018.

LAWS, E.A.; FALKOWSKI, P.G.; SMITH, W.O.; DUCKLOW, H.; MCCARTHY, J.J., Temperature effects on export production in the open ocean. **Global Biogeochemical Cycles,** 14, 1231–1246, 2000.

LEGECKIS, R. Long waves in the eastern equatorial Pacific Ocean: A view from a geostationary satellite, **Science**, v. 197, p. 1179-1181, 1977, doi: 10.1126/science.197.4309.1179.

LEGECKIS, R., PICHEL,W. AND NESTERCZUK, G. Equatorial long waves in geostationary satellite observations and in a multichannel sea surface temperature analysis, **Bulletin of the American Meteorological Society**, v. 64, p. 133-139, 1983.

LENTZ, S. J., Seasonal variations in the horizontal structure of the Amazon Plume inferred from historical hydrographic data, **Journal of Geophysical Research,** 100(C2), 2391–2400, 1995. doi:10.1029/94JC01847

LENTZ, S. J., AND R. LIMEBURNER, The Amazon River Plume during AMASSEDS: Spatial characteristics and salinity variability. **Journal of Geophysical Research,** 100, 2355–2376, 1995, doi: 0.1029/94JC01411

LIU, D. Y. AND WANG, Y. Q., Trends of satellite derived Chlorophyll *a* (1997–2011) in the Bohai and Yellow Seas, China: Effects of bathymetry on seasonal and interannual patterns, **Progress in Oceanography**., 116, 154–166, 2013.

LIU, W. T. H. **Aplicações de sensoriamento remoto**. 2. ed. ampl. São Paulo: Oficina de

Textos, 2006. p. 3-4.

LONGHURST, A.R. A review of the oceanography of the Gulf of Guinea. **Bulletin de L'InstituteFrançaisd'Afrique Noire**,v. 24, p. 633–663, 1962.

LONGHURST, A. Seasonal cooling and blooming in the tropical oceans, **Deep-SeaResearchI,** 40, 2145–2165, 1993. doi: 10.1016/0967-0637(93)90095-K.

MOLLERI S. F., GUSTAVO & NOVO, EVLYN & KAMPEL, M., Space-time variability of the Amazon River plume based on satellite ocean color. **Continental Shelf Research**. 30, 2010, doi: 10.1016/j.csr.2009.11.015.

MULLER-KARGER, F.E., MCCLAIN, C.R., RICHARDSON, P.L., The dispersal of the Amazon water. **Nature.** 333, 56–59, 1988.

MULLER-KARGER, F.E., VARELA, R.,THUNELL, R.,LUERSSEN, R., HU, C. AND WALSH, J.J. The importance of continental margins in the global carbon cycle, **Geophysical Research Letters**, v. 32, L01602, 2005. doi: 10.1029/2004GL021346.

OH, J. AND SUH, K. Real-time forecasting of wave heights using EOF – wavelet – neural network hybrid model, **Ocean Engineering**, v. 150, p. 48–59, 2018. doi:10.1016/j.oceaneng.2017.12.044.

OKUMURA, Y. AND XIE, S. Interaction of the Atlantic Equatorial Cold Tongue and the African Monsoon, **Journal of Climate**, v. 17, p. 3589–3602, 2004. doi:10.1175/1520-0442(2004)017.<3589:IOTAEC>2.0.CO;2.

O'REILLY, J.E., MARITORENA, S.,MITCHELL, B. G., SIEGEL, D. A., CARDER, K. L., GARVER, S. A., KAHRU, M., & MCCLAIN, C. R. Ocean color chlorophyll algorithms for SeaWiFS, **Journal of Geophysical Research** 103, 24937-24953, 1998. doi: 10.1029/98JC02160.

PERRY, G. D., P. B. DUFFY, AND N. L. MILLER, An extended data set of river discharges for validation of general circulation models. **Journal of Geophysical Research,** 101, 21339–21349, 1996, doi: 10.1029/96JD00932.

PETERSON, R.G. AND STRAMMA, L. Upper-level circulation in the South Atlantic Ocean, **Progress in Oceanography**, v. 26, p. 1-73, 1991, doi: 10.1016/0079-6611(91)90006-8.

PICAUT, J., Propagation of the Seasonal Upwelling in the Eastern Equatorial Atlantic. **J. Journal of Physical Oceanography**., 13, 18–37, 1983, doi: 10.1175/1520-0485(1983)013<0018:POTSUI>2.0.CO;2.

RAJEESH, R.; DWARAKISH, G. S. Satellite oceanography - A review. International Conference on Water Resources, Coastal and Ocean Engineering (ICWRCOE). **Aquatic Procedia**, v. 4, p. 165-172, 2015, doi: 10.1016/j.aqpro.2015.02.023.

REGNIER, P. *et al*., Anthropogenic perturbation of the carbon fluxes from land to ocean. **Nature Geoscience**, 6, 597–607, 2013, doi: 10.1038/ngeo1830.

RICHARDSON, P.L., HUFFORD, G.E., LIMEBURNER, R. AND BROWN, W.S. North Brazil Current retroflection eddies, **Journal of Geophysical Research**, v. 99, issue C3, p. 5081–5093, 1994. doi: 10.1029/93JC03486.

RICHARDSON, P.L. AND REVERDIN, G. Seasonal cycle of velocity in the Atlantic North Equatorial Countercurrent as measured by surface drifters, current meters, and ship drifts, **Journal of Geophysical Research**, v. 92, p. 3691–3708, 1987, doi: 10.1029/JC092iC04p03691.

RICHARDSON, P.L. AND WALSH, D. Mapping climatological seasonal variations of surface currents in the tropical Atlantic using ship drifts, **Journal of Geophysical Research**, v. 91, issue C9, p.10537–10550, 1986. doi: 10.1029/JC091iC09p10537.

RODRIGUES, R.R., ROTHSTEIN, L.M. AND WIMBUSH, M. Seasonal Variability of the South Equatorial Current Bifurcation in the Atlantic Ocean: A Numerical Study, **Journal of Physical Oceanography,** v. 37, p. 16–30, 2007, doi: 10.1175/JPO2983.1.

SATHYENDRANATH, S., COTA, G., STUART, V., MAASS, H., PLATT, T., Remote sensing of phytoplankton pigments: a comparison of empirical and theoretical approaches. **International Journal of Remote Sensing** 22 (2-3), 249-273, 2001, doi:10.1080/014311601449925.

SCHMITZ JR., W. J. On the interbasin-scale thermohaline circulation, **Reviews of Geophysics,** v. 33, p. 151–173, 1995. doi:10.1029/95RG00879.

SCHOUTEN, M.W., MATANO, R.P. AND STRUB, T.P. A description of the seasonal cycle of the equatorial Atlantic from altimeter data, **Deep-Sea Research I**, v. 52, p. 477 – 493, 2005. doi: 10.1016/j.dsr.2004.10.007.

SCHOTT, F.A., DENGLER, M., ZANTOPP, R., STRAMMA, L., FISCHER, J. AND BRANDT, P. The Shallow and Deep Western Boundary Circulation of the South Atlantic at

5°–11°S, **Journal of Physical Oceanography**, v. 35, p. 2031–2053, 2005. doi: 10.1175/JPO2813.1.

SERVAIN, J., PICAUT, J. AND MERLE, J. Evidence of remote forcing in the equatorial Atlantic Ocean, **Journal of Physical Oceanography**, v. 12, p.457–463, 1982. doi:10.1175/1520-0485(1982)012<0457:EORFIT>2.0.CO;2.

SIEGEL, D. A., S. C. DONEY, AND J. A. YODER, The North Atlantic spring phytoplankton bloom and Sverdrup's critical depth hypothesis, **Science**, 296, 730–733, 2002, 10.1126/science.1069174.

SIGNORINI, S. R., R. G. MURTUGUDDE, C. R. MCCLAIN, J. R. CHRISTIAN, J. PICAUT, AND A. J. BUSALACCHI, Biological and physical signatures in the tropical and subtropical Atlantic, **Journal of Geophysical Research**, 104(C8), 18367–18382, 1999, doi:10.1029/1999JC900134.

SILVA, A. C. DA, SANTOS, M. DE L. S., ARAUJO, M. C. AND BOURLÈS, B., Observações hidrológicas e resultados de modelagem no espalhamento sazonal e espacial da pluma de água Amazônica, **Acta Amazônica**, v.39(2): 361 – 370, 2009.

SMITH, W.O. JR., DEMASTER, D.J., Phytoplankton and biomass productivity in the Amazon river plume: correlation with seasonal river discharge. **Continental Shelf Research,** 16: 291-317, 1996.

SARMIENTO, J. L.; GRUBER, N. Ocean Biogeochemical Dynamics. Princeton: Princeton University Press, 2006.

SOLANKI, H.U., DWIVEDI, R.M., NAYAK, S.R., JADEJA, J.V., THAKAR, D.B., DAVE, H.B. & PATEL, M.I., Application of ocean colour monitor chlorophyll and AVHRR SST for fishery forecast: Preliminary validation results off Gujarat coast, northwest coast of India, **Indian Journal of Marine Science**, 30 132-138, 2001.

STRAMMA, L. AND ENGLAND, M. On the water masses and mean circulation of the South Atlantic Ocean**, Journal of Geophysical Research**, v. 104, issue C9, p. 20863–20883, 1999. doi: 10.1029/1999JC900139.

STRAMMA, L. AND SCHOTT, F. The mean flow field of the tropical Atlantic Ocean, **Deep-Sea Research II**, v. 46, p. 279–303, 1999. doi: 10.1016/S0967-0645(98)00109-X.

STRAMMA, L., RHEIN, M., BRANDT, P., DENGLER, M., BÖNING, C. AND WALTER, M. Upper ocean circulation in the western tropical Atlantic in boreal fall 2000, **Deep-Sea Research I,** v. 52, p. 221–240, 2005. doi:10.1016/j.dsr.2004.07.021.

SUDRE, J. AND MORROW, R.A. Global surface currents: A high-resolution product for investigating ocean dynamics, **Ocean Dynamics,** v. 58, p. 101–118, 2008. doi:10.1007/s10236-008-0134-9.

URBANO, D.F., DE ALMEIDA, R.A.F. AND NOBRE, P. Equatorial Undercurrent and North Equatorial Countercurrent at 38°W: A new perspective from direct velocity data, **Journal of Geophysical Research**, v. 113, C04041, 2008. doi: 10.1029/2007JC004215.

VAUTARD R., YIOU P., GHIL M. Singular spectrum analysis: a toolkit for short, noisy chootic signals. **Physical** S 58,95-126, 1992. doi: 10.1016/0167-2789(92)90103-T.

VELEDA, D., ARAUJO, M., ZANTOPP, R. AND MONTAGNE, R. Intraseasonal variability of the North Brazil Undercurrent forced by remote winds**, Journal of Geophysical Research**, v. 117, C11024, 2012. doi: 10.1029/2012JC008392.

VOITURIEZ, B., AND A. HERBLAND, Primary production in the equatorial Atlantic Ocean mapped from oxygen values of Equalant 1 and 2, Bul. Mar. **Science,** 31, 8543–863, 1981.

VON SCHUCKMANN, K., BRANDT, P. AND EDEN, C. Generation of tropical instability waves in the Atlantic Ocean, **Journal of Geophysical Research,** v. 113, C08034, 2008. doi: 10.1029/2007JC004712.

WEISBERG, R.H. AND HORIGAN, A.M. Low-frequency variability in the equatorial Atlantic, **Journal of Physical Oceanography**, v. 11, p. 913–920, 1981. doi: 10.1175/1520-0485(1981)011<0913:LFVITE>2.0.CO;2.

WILKS, D.S., Statistical methods in the atmospheric sciences: An introduction. **San Diego: Academic Press**, p. 467, 1995.

WILSON W.D., JOHNS, W.E. AND GARZOLI, S.L. Velocity structure of North Brazil Current rings, **Geophysical Research Letters**, v. 29 (8), 2002. doi: 1029/2001GL013869.

WISSER, D., FEKETE, B. M., VÖRÖSMARTY, C. J. AND SCHUMANN, A. H., Reconstructing 20th century global hydrography: a contribution to the Global Terrestrial

Network- Hydrology (GTN-H). **Hydrology and Earth System Sciences,** 14, 1–24, 2010, doi:10.5194/hess-14-1-2010.

YODER, J.A. AND KENNELLY, M.A. Seasonal and ENSO variability in global ocean phytoplankton chlorophyll derived from 4 years of SeaWiFS measurements, **Global Biogeochemichal Cycles**, v. 17, 1112, 2003. doi: 10.1029/2002GB001942, 4.

YODER, J.A. AND KENNELLY, M.A., What have we learned about ocean variability from satellite ocean color images?,**Oceanography**, 19152-171, 2006, doi: 10.5670/oceanog.2006.98.